R-05-05

Bedrock transport properties

Preliminary site description Simpevarp subarea – version 1.2

Johan Byegård, Eva Gustavsson, Geosigma AB

Eva-Lena Tullborg, Terralogica AB

Sten Berglund, Svensk Kärnbränslehantering AB

June 2005

Svensk Kärnbränslehantering AB
Swedish Nuclear Fuel
and Waste Management Co
Box 5864
SE-102 40 Stockholm Sweden
Tel 08-459 84 00
+46 8 459 84 00
Fax 08-661 57 19
+46 8 661 57 19

ISSN 1402-3091
SKB Rapport R-05-05

Bedrock transport properties

Preliminary site description Simpevarp subarea – version 1.2

Johan Byegård, Eva Gustavsson, Geosigma AB

Eva-Lena Tullborg, Terralogica AB

Sten Berglund, Svensk Kärnbränslehantering AB

June 2005

Keywords: Retardation model, Transport properties, Simpevarp, Fracture mineralogy, Diffusivity, Porosity, Sorption.

Abstract

This report presents the site descriptive model of transport properties developed as a part of the Simpevarp 1.2 site description. The main parameters included in the model, referred to as retardation parameters, are the matrix porosity and diffusivity, and the matrix sorption coefficient K_d. The model is based on the presently available site investigation data, mainly obtained from laboratory investigations of core samples from boreholes within the Simpevarp subarea, and on data from previous studies at the Äspö Hard Rock Laboratory (Äspö HRL). The modelling is a first attempt, based on limited data, to obtain a description of the retardation parameters. Further refinement of the model is foreseen when more data becomes available for future versions of the Simpevarp site description.

The modelling work included descriptions of rock mass geology, the fractures and deformation zones, the hydrogeochemistry and also the available results from the site specific porosity, sorption and diffusivity measurements. The description of the transport-related aspects of the data and models presented by other modelling disciplines is an important part of the transport description. In accordance with the strategy for the modelling of transport properties, the results are presented as a "retardation model", in which a summary of the transport data for the different geological compartments is given.

Concerning the major rock types, Ävrö granite, quartz monzodiorite and fine-grained dioritoid are identified as the rock types dominating the main rock domains identified and described in the site descriptive model of the bedrock geology. However, relatively large parts of the rock consist of altered rock and the open fracture frequency appears to be correlated to the altered/oxidised parts of the rock. This implies that transport in open fractures to a large extent takes place in the altered parts of the rock. For the fracture mineralogy, it is found that the hydraulically conductive structures are mostly associated with the presence of gouge-filled faults. The mineralogy of the different fracture coatings cannot be correlated to their corresponding host rock type.

The hydrogeochemistry has been included in the model by identifying four different groundwater types: (I) fresh diluted Ca-HCO_3 water present in the upper 100 m of the bedrock, (II) groundwater with marine character (Na-(Ca)-Mg-Cl, 5,000 mg/L Cl), (III) groundwater of Na-Ca-Cl type (8,800 mg/L Cl), i.e. present groundwater at repository level in the Simpevarp peninsula, and (IV) brine type water of very high salinity (Ca-Na-Cl type water with Cl content of 45,000 mg/L).

The retardation data included in the present model are porosities, diffusivities (expressed in terms of formation factors) and sorption coefficients for intact (non-altered) and altered varieties of the rock types at Simpevarp. Porosities and formation factors have been measured for the major rock types using site specific materials from the Simpevarp area. Mean values for the major rock types have been obtained in the range of 0.17–0.40 vol-% for the porosity and 1.0×10^{-4}–2.9×10^{-4} for the formation factor. Due to lack of site specific sorption data, K_d-values have been imported from previous investigations of Äspö diorite at Äspö HRL. This import was justified on the basis of the mineralogical similarity of the major rock types of the Simpevarp site and the Äspö diorite. Only K_d for the Sr^{2+} and Cs^+ interaction in a groundwater of type III were available; values of 4.2×10^{-5} m^3/kg (Sr^{2+}) and 0.06 m^3/kg (Cs^+) were given.

The descriptions of bedrock geology and fracture mineralogy are used as a basis for identifying a set of fracture types considered typical for the boreholes in the Simpevarp subarea. Four fracture types were identified and described in terms of geometry (thicknesses of different layers) and retardation parameters. Due to the present lack of data, no deformation zone types could be included in the model. Tables describing the retardation parameters assigned to each major rock type and each fracture type are presented. However, it is acknowledged that there is a lack of retardation data in the present stage of the site descriptive modelling. In particular, the current site investigation database contains no site-specific sorption data or retardation data on the fracture materials.

Sammanfattning

I denna rapport ges den beskrivande modellen för transportparametrarna vilka är avsedda att användas i Simpevarp platsbeskrivning, version 1.2. De parametrar som inkluderats i modellen, angivna som retardationsparametrar, är matrisporositeten och diffusiviteten, samt sorptionskoefficienten K_d. Modellen baseras på i nuläget tillgänglig platsundersökningsdata, huvudsakligen erhållen från laboratorieundersökningar av borrkärneprover från borrhål i Simpevarpsområdet, och data från tidigare studier på material provtaget i det närbelägna Äspö Hard Rock Laboratory (Äspö HRL). Modelleringen är ett första försök att, utifrån den begränsade mängden tillgängliga data, utföra en beskrivning av de aktuella retardationspar ametrarna. En mer detaljerad modell kan förväntas i de framtida platsbeskrivningarna då en större mängd platsspecifik data kommer att vara tillgänglig.

Modelleringsarbetet innehåller beskrivningar av berggrundsgeologin, sprickor och deformationszoner, hydrogeokemiska data och även de i nuläget tillgängliga data från de platsspecifika mätningarna av porositet, diffusivitet samt sorptionskoefficienter. Beskrivningar av transportrelaterade aspekter av data och modeller som givits av andra modelleringsdiscipliner är också en viktig del av transportbeskrivningen. I enlighet med strategin för modelleringen av transportegenskaper presenteras resultaten i form av en ”retardationsmodell”, i vilken en summering ges av transportdata för de olika geologiska enheterna.

Ävrögranit, kvartsmonzodiorit samt finkorning dioritoid har identifierats som huvudbergarter i de bergdomäner som identifierats och beskrivits i den platsbeskrivande modellen av berggrundsgeologin. Dock utgörs stora delar av berggrunden av omvandlat bergmaterial och frekvensen av öppna sprickor förefaller vara korrelerad till förekomsten av omvandlat och oxiderat bergmaterial. Detta medför att transport i öppna sprickor till stor del sker i berg innehållande omvandlat material. Vad beträffar sprickmineralogin kan det konstateras att hydrauliskt ledande strukturer huvudsakligen karaktäriseras av närvaro av sprickfyllnadsmaterial (fault gouge). Sprickmineralernas sammansättning går dock inte att enkelt korrelera till de huvudbergarter som dessa sprickor går igenom.

Variationerna i hydrogeokemin på platsen har adresserats genom en identifiering av fyra olika grundvattentyper: (I) icke-salint utspätt Ca-HCO_3 vatten, förekommande i de övre 100 m av berggrunden, (II) grundvatten med marin karaktär (Na-Ca-Mg-Cl, 5 000 mg/L Cl), (III) grundvatten av Na-Ca-Cl typ (8 800 mg/L Cl), förekommande på förvarsdjup på Simpevarpshalvön samt (IV) grundvatten med ”brine” karaktär (Ca-Na-Cl grundvattentyp med Cl-innehåll på 45 000 mg/L).

De retardationsdata som denna modell innehåller är porositet, diffusivitet (uttryckt som formationfaktor) och sorptionskoefficienter för icke-omvandlade och omvandlade bergarter i Simpevarp. Porositeter and formationsfaktorer har mätts för huvudbergarterna på platsspecifika prover från Simpevarpområdet. Medelvärden för huvudbergarterna har erhållits i intervallen 0,17–0,40 vol-% för porositet och $1{,}0\times10^{-4}$–$2{,}9\times10^{-4}$ för formationsfaktorn. På grund av bristen på platsspecifikt mätta sorptionsdata har K_d-värden importerats från tidigare undersökningar av Äspödiorit provtagen i Äspö HRL. Denna import motiverades med den mineralogiska likheten mellan Simpevarps huvudbergarter och Äspödioriten. Endast K_d för spårämnena Sr^{2+} och Cs^{+} i ett system med grundvatten av typ III fanns tillgängliga och värden på $4{,}2\times10^{-5}$ m^3/kg (Sr^{2+}) och 0,06 m^3/kg (Cs^{+}) angavs för dessa system.

Beskrivningen av berggrundsgeologin och sprickmineralogin användes för att identifiera ett antal typsprickor som ansågs representativa för borrhålen i Simpevarpsområdet. Fyra olika spricktyper identifierades och beskrevs i termer av geometrier (tjockleken av de olika skikten) och retardationsparametrar. På grund av bristen på platsspecifik data kunde ingen klassificering av deformationszoner inkluderas i modellen. Tabeller som beskriver retardationsparametrar gavs för varje huvudbergart och för varje spricktyp. Bristen på platsspecifika data, särskilt avseende sorptionen och avseende samtliga retardationsparametrar i vattenförande zoner, är dock identifierad som en allmän svaghet i denna version av i transportmodellen för Simpevarp.

Contents

1 Introduction

1.1 Background

The Swedish Nuclear Fuel and Waste Management Company (SKB) is conducting site investigations at two different locations, the Forsmark and Simpevarp areas, with the objective of siting a geological repository for spent nuclear fuel. The results from the investigations at the sites are used as a basic input to the site descriptive modelling.

A Site Descriptive Model (SDM) is an integrated description of the site and its regional setting, covering the current state of the geosphere and the biosphere as well as ongoing natural processes of importance for long-term safety. The SDM shall summarise the current state of knowledge of the site, and provide parameters and models to be used in further analyses within Safety Assessment, Repository Design and Environmental Impact Assessment. The present report is produced as a part of the version 1.2 modelling of the Simpevarp area.

The process of site descriptive modelling of transport properties is described by /Berglund and Selroos, 2004/. Essentially, the description consists of three parts:

- Description of rock mass and fractures/deformation zones, including relevant processes and conditions affecting radionuclide transport; the description should express the understanding of the site and the evidence supporting the proposed model.
- Retardation model: Identification and description of "typical" rock materials and fractures/deformation zones, including parameterisation.
- Transport properties model: Parameterisation of the 3D geological model and assessment of understanding, confidence and uncertainty.

The methods used within the transport programme produce primary data on the retardation parameters, i.e. the porosity, θ_m, the effective diffusivity, D_e, and the linear equilibrium sorption coefficient, K_d. These retardation parameters are evaluated, interpreted and presented in the form of a retardation model; the strategy for laboratory measurements, data evaluation and development of retardation models is described by /Widestrand et al. 2003/. In the three-dimensional modelling, the retardation model is used to parameterise the various geological "elements" (rock mass, fractures and deformation zones) in the site descriptive geological model.

1.2 Conceptual model with potential alternatives

1.2.1 Basic conceptual model

The conceptual model underlying the site descriptive transport modelling is based on a description of solute transport in discretely fractured rock. Specifically, the fractured medium is viewed as consisting of mobile zones, i.e. fractures and deformation zones where groundwater flow and advective transport take place, and immobile zones in rock mass, fractures and deformation zones where solutes can be retained, i.e. be removed, temporally or permanently, from the mobile water /Berglund and Selroos, 2004/.

In the safety assessment framework that provides the basis for identification of retention parameters in the site descriptive models, retention is assumed to be caused by diffusion and linear equilibrium sorption. These processes are reversible and are here referred to as retardation processes.

The conceptualisation outlined above implies that radionuclide transport takes place along flow paths consisting of connected "subpaths" in fractures and deformation zones of different sizes. In this model, advection is the dominant process for moving the radionuclides in the transport direction, whereas the main role of diffusion is to remove the solutes from the mobile zone and transport them within the immobile zones. It should be noted that this conceptual model and the present methodology for site descriptive modelling in general are based on experiences from the Äspö Hard Rock Laboratory (Äspö HRL), primarily the Tracer Retention Understanding Experiment (TRUE) project /Winberg et al. 2000; Poteri et al. 2002/ and the Äspö Task Force on modelling of groundwater flow and transport of solutes, e.g. /Dershowitz et al. 2003/, which are not necessarily fully applicable to the transport conditions at the Simpevarp site. This is to say that the modelling strategy and the basic conceptual model could be revised as a result of experiences gained in the site descriptive modelling.

1.2.2 Alternative processes and process models

Alternative conceptual models could involve additional processes and/or more refined descriptions of the presently considered processes. Furthermore, different conceptualisations of the radionuclide transport paths, i.e. as advective flow paths in accordance with the basic conceptual model described above or with, for instance, diffusive transport in the mobile zone, could be considered. For radionuclide retention, consideration of more refined representations of sorption (process-based sorption models) and additional retention processes (e.g. precipitation and co-precipitation) are of particular interest.

Modelling activities involving process-based sorption models have been initiated during the S1.2 transport modelling. This modelling constitutes a first attempt at reactive-transport simulations in a single fracture, using data from Äspö HRL /Dershowitz et al. 2003/. The aims are to gain experience of this type of modelling in a transport context and to investigate whether the process-based sorption models show qualitative differences or specific features that cannot be reproduced with K_d-based models. Whereas such differences and features can be observed in the presently available results, it remains to be evaluated whether these effects are important and may occur under realistic conditions. Hence, no conclusive results that could support, or provide alternatives to, the K_d-based model presented here are currently available.

1.3 Transport modelling in Simpevarp 1.1

The Simpevarp 1.1 (S1.1, for brevity) modelling of transport properties is described in /SKB, 2004a/. The main uncertainty identified in the 1.1 stage was related to the fact that no site investigation transport data were available. As further discussed below, this uncertainty is only partly resolved in the Simpevarp 1.2 (S1.2) model.

The S1.1 modelling was focused on an evaluation of transport data from research projects at Äspö HRL and their potential use within the site descriptive modelling. However, the complete version 1.1 geological model was not available at the time for the transport modelling. Based on the limited geological comparisons that could be made, it was concluded that the diffusion and sorption data from Äspö HRL provided information on

only one of the main rock types (quartz monzodiorite, interpreted as equivalent to Äspö diorite) and one of the less frequent rock types (fine-grained granite) within the Simpevarp area. The potential for further "import" of data from Äspö HRL has been investigated in the present model version.

The version 1.1 modelling considered intact rock only; no attempt was made to relate transport data from fractures and deformation zones on Äspö HRL to those within the Simpevarp area. For the intact rock, the results of the 1.1 modelling, which also included a comparison with the SR 97 databases /Ohlsson and Neretnieks, 1997; Carbol and Engkvist, 1997/, emphasised the need for site-specific data on the diffusion properties of, in particular, the fine-grained dioritoid, and on sorption properties of site-specific materials in general.

1.4 Parameters presented in the Simpevarp 1.2 model

The strategy for site descriptive modelling of transport properties has been modified between model versions 1.1 and 1.2. In version 1.2, flow-related transport parameters are not presented as a part of the site descriptive transport model. This implies that all calculations of flow-related transport parameters, including quantifications of retention variability along flow paths, will be handled by Safety Assessment, whereas the site descriptive model is focused on the retardation parameters and their representation within the framework of the geological site descriptive model.

The main reasons for this change in strategy is the experience gained during and after the version 1.1 modelling, in combination with the fact that Simpevarp 1.2 does not include more detailed groundwater flow modelling than the previous model version. Specifically, it was found difficult to communicate, internally as well as externally, the difference between "F-values" and travel times (t_w) obtained from the large-scale flow models in the site descriptive modelling, and the "actual performance measures", also expressed in terms of F and t_w, that were calculated with the higher-resolution flow models (including repository layouts) developed by Safety Assessment.

1.5 This report

The aim of the present report is to give a description of the development of the Simpevarp 1.2 retardation model, and to give the background and the data that are used for the justification of the retardation model. Thus, the report focuses primarily on the first and second bullet points in the strategy outlined in Section 1.1. The data and models used as input to the modelling are described in Chapter 2, including the inputs from other modelling disciplines. Chapter 3 presents the evaluation of Transport data, whereas the resulting model is described in Chapter 4. Finally, Chapter 5 contains a summary and a brief discussion on the implications of the results for the continued investigations and modelling.

2 Description of input data

2.1 Summary of available data

The input data to the Simpevarp 1.2 modelling of transport properties are summarised in Table 2-1. The available site investigation data on transport properties are described by /Gustavsson and Gunnarsson, 2005/ and /Löfgren and Neretnieks, 2005/. The important input from joint geological/hydrogeochemical interpretations of fracture mineralogy and wall rock alteration data is provided by /Drake and Tullborg, 2004/. As shown in Table 2-1, other geological, hydrogeological and hydrogeochemical inputs were obtained from the SDM report, i.e. from draft versions of the relevant chapters, and from the hydrogeochemical modelling background report /SKB, 2004b/. These inputs are further detailed below.

Table 2-1. Available data on transport properties and input data from other disciplines, and their handling in Simpevarp 1.2 (S1.2).

Available primary data data specification	Ref.	Usage in S1.2 analysis/ modelling	Not utilised in S1.2 arguments/comments
Cored borehole data			
Formation factors measured *in situ* and in the laboratory, KSH01A and KSH02	P-05-27 SICADA	Assignment of porosity and diffusion parameters	
Results from through-diffusion tests and porosity measurements on samples from KSH01A and KSH02	P-05-18 SICADA	Assignment of porosity and diffusion parameters	
Input from other disciplines			
Geological data and description:			
– lithology and mineralogy of identified rock types – fracture mineralogy – porosity data from surface samples and boreholes (KSH01A, KSH02)	SDM chapter P-04-102 P-04-250 P-03-97 P-04-28 P-04-77	Identification of site-specific rock types, fractures and deformation zones, and properties of site-specific geological materials, as a basis for Retardation model and descriptive Transport model	
Hydrogeological data and description	SDM chapter P-03-70 P-03-110	Identification of conductive fractures and correlations between fracture types and hydraulic properties	
Hydrogeochemical data and description	SICADA R-04-74	Identification of site-specific water types and water-rock interactions	
Other borehole data and models			
Data and models from TRUE project and Äspö Task Force (Task 6C)	TR-98-18 ICR-01-04 IPR-03-13	Conceptual modelling Assignment of sorption and diffusion parameters	Some old data not used due to differences in methods and/or insufficient sample characterisation
Data from other research at Äspö HRL and Laxemar	SKI 98:41 Research papers	Assessment of spatial variability	Discussed in S1.1
SR 97 sorption and diffusion databases	R-97-13 TR-97-20	Used for comparative purposes	Discussed in S1.1

2.2 Data and models from other disciplines

2.2.1 Geology

The following summary and evaluation of geological data of relevance for the transport modelling is based on the S1.2 geological description, as presented in Chapter 5 of the S1.2 SDM report /SKB, 2005/, and the associated models and databases. Specifically, the geological models were delivered in August 2004, and a draft version of the geological description (i.e. Chapter 5 in the SDM report) was made available for the Transport modelling.

Igneous rocks that belong to the c 1,800 Ma generation of the Transscandinavian Igneous Belt (TIB) dominate in the Simpevarp regional and local scale model areas. As described in /SKB, 2005/, magma mixing and mingling and diffuse contact relationships is a characteristic feature of these rocks, which show compositions varying from true granites to quartz monzodiorite. The granidioritic and quartz-monzodioritic compositions dominate in the Simpevarp area, and the following three rock types make up most of the local area: Ävrö granite (usually porphyritic in texture and with composition ranging from granite to quartz monzodiorite), quartz monzodiorite (medium-grained) and fine-grained dioritoid. The properties and characteristics of these rock types are given in tables in /SKB, 2005/.

The fine-grained dioritoid dominates in the southern part of the Simpevarp peninsula. Minor rock types, most of which are additional varieties of rocks belonging to the TIB suite, occur as dikes, lenses and xenlithes; these are fine-grained granite, medium- to coarse-grained granite, pegmatite, fine-grained diorite to gabbro, and equigranular diorite to gabbro. Figure 2-1 shows the bedrock map of the Simpevarp subarea. In the regional model area, a 1,450 Ma old granite occurs in two major bodies, one in the northern and one in the southern part of the model area.

Within the Simpevarp subarea, five core-drilled boreholes have been performed: KSH01, KSH02 and KSH03 on the Simpevarp peninsula, and KAV01 and KAV04 on the Ävrö island. Of these boreholes, only those on the Simpevarp peninsula have been sampled for laboratory investigations of transport parameters and fracture mineralogy, and only KSH01 for a full hydrogeochemical characterisation /SKB, 2004b/. Therefore, only the three boreholes on the Simpevarp peninsula are discussed in the following sections.

An overview of rock types, alteration and frequencies of sealed and open fractures in the Simpevarp boreholes is given in the S1.2 SDM report /SKB, 2005/. In these results, it can be observed that the frequency of sealed fractures does not always correlate with the frequency of open fractures. However, the open fracture frequency seems to be correlated with the altered and oxidised parts of the bedrock. This implies that transport and retention along the open fractures will, to large extent, take place in altered wall rock.

From the geological map and the borehole loggings it is obvious that, on a detailed scale, there is a mix of rock types. For the lithological modelling of the area, the concept of rock domains is introduced in order to facilitate the development of a three-dimensional geological model of the area. Three rock domains build up the Simpevarp peninsula and these are assigned properties, comprising mineralogical composition, grain size, texture, density, porosity, etc /SKB, 2005; Table 5-13/. The lithological model and the parameters assigned to each rock domain are summarised in Chapter 11 of the SDM report (cf Tables 11-1 to 11-3); the proportions of different rock types within the rock domains are illustrated in Figures 5-45 to 5-47 in /SKB, 2005/.

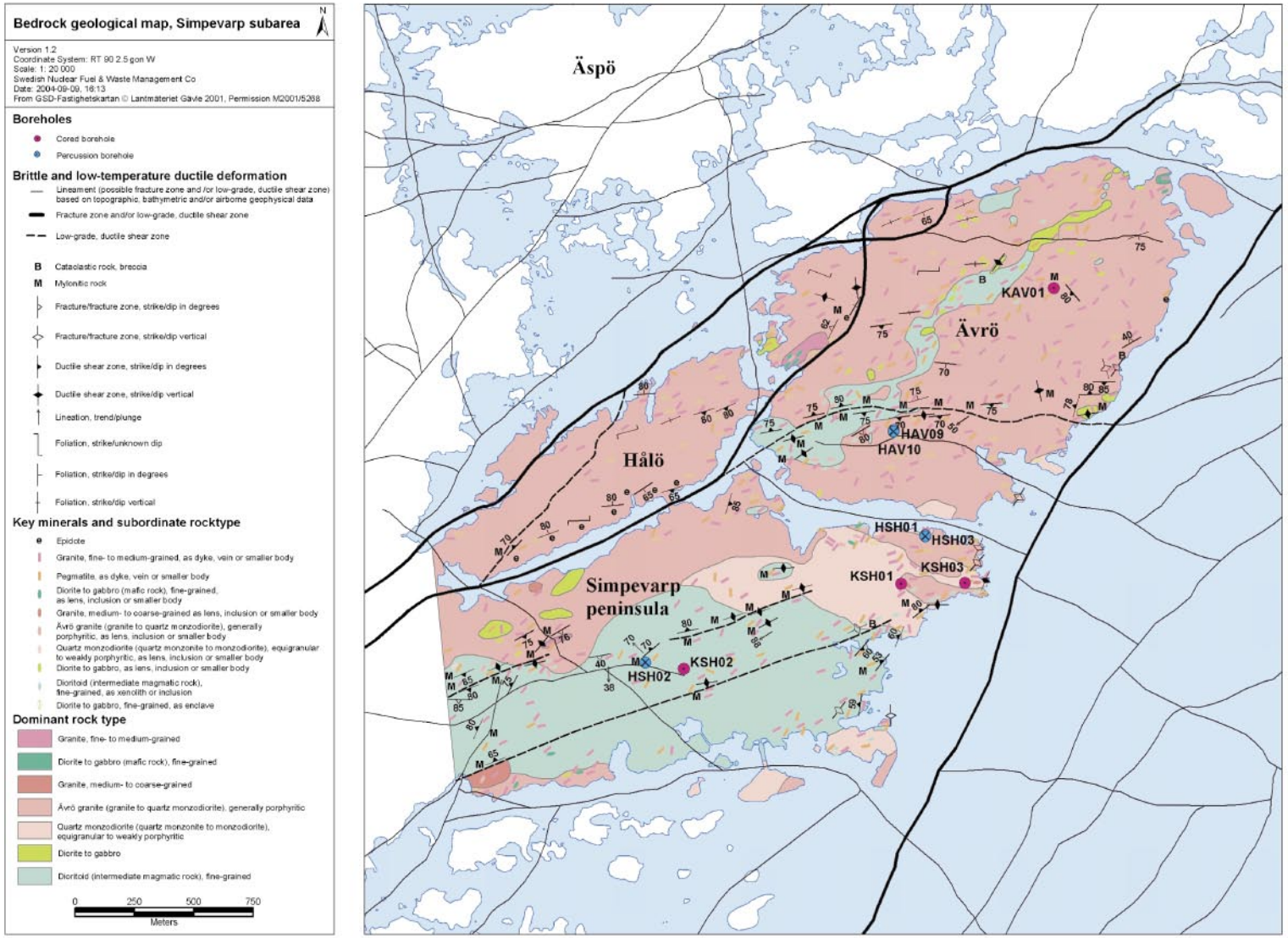

Figure 2-1. *Map of bedrock geology in the Simpevarp subarea.*

The three rock domains are:

RSMA01 = dominantly Ävrö granite

RSMB01 = dominantly fine-grained dioritoid

RSMC01 = 50% Ävrö granite and 50% quartz monzodiorite

Hydrothermal alteration/oxidation of the host rock along the fractures is a common feature in the entire regional area, but is especially frequent and widespread at the Simpevarp peninsula. Figures 5-49 to 5-51 in /SKB, 2005/ show the volume of altered rock compared to the fresh rock. Four different degrees of alteration are used in the core logs: faint, weak, medium and strong. As shown in the figures, and summarised in Table 2-2 below, relatively large parts of the different rock domains at the Simpevarp peninsula and Ävrö are affected by this alteration. However, large variations in intensity between boreholes are recorded; e.g. KSH03A shows a very high alteration intensity in the upper part of the borehole.

The cause of the observed red-staining of the rock is hydrothermal alteration/oxidation, which has resulted in saussuritisation of plagioclase, breakdown of biotite to chlorite and oxidation of Fe(II) to form hematite, mainly present as micro-grains giving the red colour. However, there is not always a perfect correspondence between the extent of hydrothermal alteration and the extent of red-staining /Drake and Tullborg, 2004/. The altered parts of the rock can be assumed to have different transport properties due to, e.g. lower biotite content and partly higher content of sericite and illite (influencing the sorption capacity), and usually higher porosity and possible also changed structure of the porosity (influencing the diffusivity). It is therefore an important consideration that the major rock types in all three domains show alteration (rated as weak/medium/strong) in 13% of the rock mass, or more.

Table 2-2. Alteration/red-staining in the different rock domains. The alteration is classified into four classes: faint, weak, medium and strong.

Rock domain	Fresh (%)	Faint (%)	Weak (%)	Medium (%)	Strong (%)
RSMA01 Dominantly Ävrö granite	65–69	13–17	14–17	0.5–5	0–0.3
RSMB01 Dominantly fine-grained dioritoid	58–68	9–23	5–13	3–14	3–6
RSMC01 50% Ävrö granite 50% quartz monzodiorite	10–78	3–51	11–35	3–5	0–6

2.2.2 Fractures and deformation zones

Fracture minerals are initially documented during the mapping of the drill core according to the boremap programme, which forms an integral part of the site characterisation protocol. Based on this information, fracture fillings are further selected for more detailed studies, which involve X-ray diffractometry for identification of clay minerals and fault gouge materials, and microscopy of fracture fillings. Samples are also selected for isotopic analyses of calcites and pyrites, and fracture fillings from water conducting fractures are sampled for U series analyses.

The most common fracture minerals at the Simpevarp site are chlorite and calcites, which occur in several different varieties and are present in most of the open fractures. Other common minerals are epidote, prehnite, laumontite, quartz, adularia (low-temperature

K-feldspar), fluorite, hematite and pyrite. A Ba-zeolite named harmotome has been identified in some fractures and apophyllite has been identified in a few diffractograms. Gypsum (small amounts) has been found in two fractures in KSH03 /Drake and Tullborg, 2004/. A compilation of the available fracture mineral results is presented in the hydrogeochemical modelling report for Simpevarp 1.2 /SKB, 2004b; Appendix 1/.

Clay minerals identified are, in addition to chlorite, corrensite (mixed layer chlorite/smectite or chlorite/vermiculite clay, the smectite or vermiculite layer are swelling), illite, mixed-layer illite/smectite (swelling) and a few observations of smectites. It can be concluded that the amounts of clay minerals are under-estimated in the core logs, mainly due to difficulties in determining clay minerals macroscopically when mixed with other minerals. Conclusions of importance for the transport modelling, mainly based on /Drake and Tullborg, 2004/ are:

1) It has so far not been possible to relate different fracture minerals to different fracture generations (in accordance with earlier findings by /Munier, 1993/).
2) The sequence of mineral paragenesis shows the transition from epidote facies in combination with ductile deformation, over to brittle deformation and breccia sealing during prehnite facies and subsequent zeolite facies. A further decreasing formation temperature series indicates that the fractures were initiated relatively early in the geological history of the host rock and have been reactivated during several different periods of various physiochemical conditions.
3) The locations of the hydraulically conductive fractures are mostly associated with the presence of gouge filled faults produced by brittle reactivation of earlier ductile precursors or hydrothermally sealed fractures. The outermost coatings along the hydraulically conductive fractures consist mainly of clay minerals, usually illite and mixed layer clays (corrensite = chlorite/smectite and illite/smectite), together with calcite and minor grains of pyrite.
4) Isotopic evidence from the calcites (KSH01A+B) indicates that the upper part of the bedrock is far more hydraulically conductive than the deeper part (> 300 m depth), and that these conditions have prevailed for a very long time. The number of open fractures at depths > 300 m and the amounts of calcites within these fractures are small. So far, however, no conclusive evidence of a strong depth dependence of the hydraulic properties of the rock has been obtained from the hydrogeological investigations /SKB, 2005; Chapter 8/. The stable isotope ratios give support for a decreased interaction with biogenic carbonate at depth larger than 300 m in KSH01A. The morphology of the calcites grown in open fractures shows crystal shapes typical for brackish or saline water carbonates (with one exception). This is in agreement with the present groundwater chemistry where saline waters (< 5,000 mg/L) are sampled already at depths of about 150 m.

For the use of the fracture description in the transport modelling, a statistical overview is needed. This input can only be obtained from the core logging. Most of the open fractures contain chlorite and calcite (cf Table 2-3). Other hydrothermal Al-silicates like prehnite, epidote and adularia are common but subordinate and are not expected to give significant contributions to the sorption capacity. Clay minerals and hematite, in contrast, are expected to have comparably higher sorption capacities, and for this purpose the percentages of these fracture coatings in the open fractures are given as well. The Ca-zeolite laumontite is found in many fractures in the area, and zeolites may have high sorption capacity. Therefore, the frequency of laumontite has been evaluated as well (Table 2-3).

Table 2-3. Total number of open fractures in boreholes KSH01A, KSH02 and KSH03A, and the percentages of fractures coated with chlorite+calcite, hematite, clay minerals and laumontite. The percentage of open fractures hosted in altered host rock is also shown.

Borehole	Total number of open fractures	Chlorite and calcite %	Hematite %	Clay minerals %	Laumontite %	% of open fractures hosted in altered wall rock
KSH01A	2,176	92	19	2.7	1.9	46
KSH02	3,789	96	19	1.0	0.5	53
KSH03A	2,172	84	42	4.1	1.5	68

The figures presented in Table 2-3 give only the frequencies of fractures where the listed minerals have been found, and not the amounts of the minerals in the fractures. Generally, hematite is always mapped and the amount in the fracture is easily overestimated due to the strong colouration produced by the ferric oxides/hydroxides. Clay minerals, in contrast, are very often underrepresented, as already discussed, and the figures should be treated as an absolute minimum. Concerning the percentages of fractures hosted in altered rock, also these should be regarded as minimum figures. Since most fractures in the area have hydrothermal minerals, they most probably also have some hydrothermal alteration in the close wall rock. This alteration may not always have produced significant red-staining, which means that the fractures were not mapped as altered even though they contain altered materials.

For the sampling of fracture coatings for batch sorption measurements, the following approach has been taken: fracture coatings representing chlorite+calcite constitute the base, and fractures containing these two minerals in addition to other minerals of interest have been selected in order to determine the importance of some common fracture minerals. Therefore five different coatings have been selected:

1. Chlorite+calcite ± adularia ± epidote ± prehnite
2. Chlorite+calcite+hematite
3. Chlorite+calcite+clay minerals
4. Chlorite+calcite+zeolite (laumontite)
5. Laumontite+calcite

Figure 2-2. *Fracture planes with chlorite+calcite and prehnite (left), and chlorite+calcite and hematite (right).*

The fifth type of coating (laumontite+calcite) is not so frequent in the Simpevarp subarea, but much more important in the Laxemar area where it occurs in large volumes, e.g. in the "Mederhult zone". The strategy is to test the above listed five fracture coating types in terms of sorption, and after that, if possible, reduce the laboratory programme by concentrating on fewer coatings (perhaps to three or four coating types).

Within the Geology programme, a number of deterministic deformation zones have been identified. These zones are large (> 1 km in length) and of regional significance; one example is the zone at 200–300 m core length in borehole KSH03A (ZSMNE024A). This zone has a very long section with severely altered rock with several sections of cataclasite and also dm-wide sections of poorly lithified fault gouge material consisting of crushed and altered rock fragments together with clay minerals and hematite.

For the modelling of radionuclides retardation, the character of the fractures/deformation zones constitutes the link between the single fractures (discussed above) and large-scale zones like ZSMNE024A. In order to ascribe realistic retardation capacities to the local minor deformation zones, the following approach has been adopted in the selection of samples. Each zone is assumed to be built up of one or several types of altered wall rock. The conductive parts of the zones usually consist of several fractures that can be referred to some of the fracture types listed above, or to a broader fault gouge-filled section. Therefore, four types of altered rocks have been selected for porosity, diffusion and batch-sorption measurements, see Figure 2-3. The present separation between single fractures and local minor deformation zones should be considered as a preliminary proposal, and will probably be the subject of discussions among hydrogeologists, geologists and transport modellers.

2.2.3 Hydrogeochemistry

The hydrogeochemical modelling of the Simpevarp subarea is based on data from KSH01A, KSH02 and KSH03A, in addition to the percussion boreholes used for supply of drilling fluid (HSH02 and HSH03). The results are presented in Chapter 9 of the S1.2 SDM report /SKB, 2005/; a more detailed description is given in /SKB, 2004b/. The overall understanding of the groundwater system at Simpevarp and Laxemar is summarised in Figure 2-4.

Water of salinity close to the one measured at repository depth has been used for the diffusivity measurements. A water composition (described as type III below) was chosen; however, only the major components (i.e. Ca^{2+}, Na^{+}, Cl^{-} and SO_4^{2-}) were included for the diffusion experiments.

For the batch sorption experiments, the groundwater composition is considered to be more important, and four different groundwater compositions have therefore been selected, as follows:

I. Fresh diluted Ca-HCO_3 water; groundwater now present in the upper 100 m of the bedrock, but also a water type that can be found at larger depths at inland sites and during late phases of glacial periods.

II. Groundwater with marine character, Na-(Ca)-Mg-Cl (5,000 mg/L Cl); a possible transgression of the Baltic Sea may introduce this type of water to repository depth.

III. Groundwater of Na-Ca-Cl type (8,800 mg/L Cl); present groundwater at repository level in the Simpevarp peninsula.

IV. Brine type water of very high salinity, Ca-Na-Cl type water with Cl content of 45,000 mg/L; during a glacial period, brine type waters can be forced to more shallow levels than at present.

1. Fault gouge

Mineralogy: chlorite, clay minerals, hematite with fragments of quartz, epidote and calcite.

Strong fragmentations.

2. Chlorite

Mineralogy: chlorite and clay minerals.

3. Porous episyentic wall rock

Mineralogy: prehnite, adularia, quartz, calcite ± laumontite, epidote, hematite.

Partly mobilized quartz.

4. Cataclasite

Cataclasite with mylonitic banding. Mineralogy: epidote, adularia, quartz, hematite.

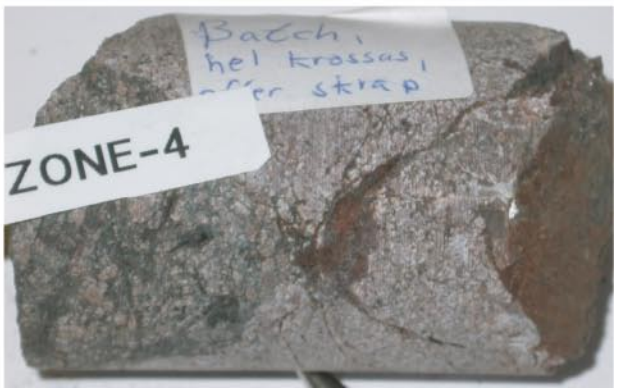

Figure 2-3. *Fracture classification for the Simpevarp site.*

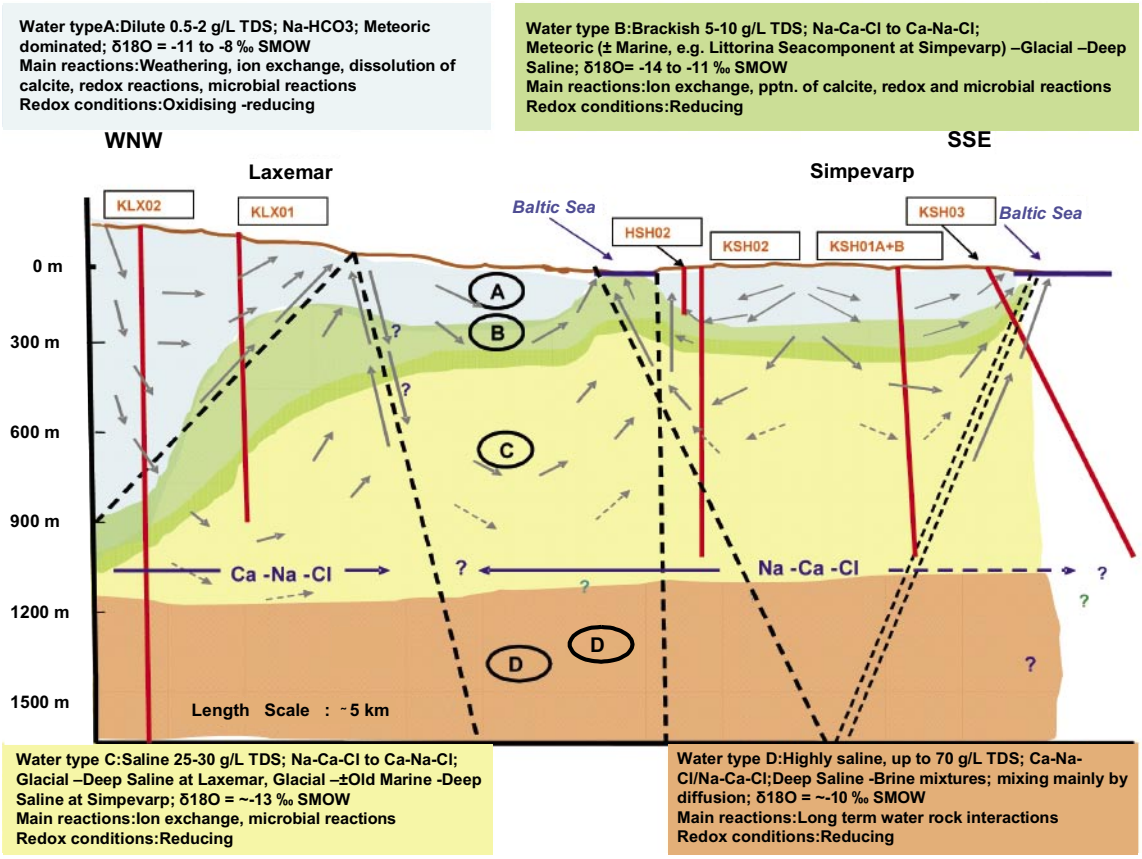

Figure 2-4. *Conceptualisation of the groundwater types identified in a transect from Laxemar to Simpevarp /SKB, 2004b/.*

The compositions of these groundwater types are specified in Table 2-4 below, referring to specific sampling intervals in the Simpevarp boreholes.

Table 2-4. Water classification of the Simpevarp area; concentrations are given in mg/L.

	Type I (HSH02 0–200m)	Type II (KFM02A 509–516m)	Type III (KSH01A 558–565m)	Type IV (KLX02 1,383–1,392m)
	Fresh water	Groundwater with marine character	Present groundwater at repository level	Brine type water of very high salinity
Li^+	1.60E–02	5.10E–02	5.80E–01	4.85E+00
Na^+	1.27E+02	2.12E+03	3.23E+03	7.45E+03
K^+	2.16E+00	3.33E+01	1.24E+01	3.26E+01
Rb^+	(2.52E–02)[A]	6.28E–02	4.24E–02	1.78E–01
Cs^+	(1.17E–03)[A]	1.79E–03	1.37E–03	1.86E–02
NH_4^+	(9.47E–02)[A]	4.00E–02	4.00E–02	5.60E–01
Mg^{2+}	1.43E+00	2.32E+02	4.47E+01	1.20E+00
Ca^{2+}	5.21E+00	9.34E+02	2.19E+03	1.48E+04
Sr^{2+}	6.95E–02	7.95E+00	3.23E+01	2.53E+02
Ba^{2+}	(1.29E+00)[A]	1.88E–01	1.88E–01	2.40E–02
Fe^{2+}	(3.64E–01)[C]	1.20E+00	6.86E–01	3.45E+00
Mn^{2+}	2.00E–02	2.12E+00	4.60E–01	1.11E+00
F^-	3.03E+00	9.00E–01	9.67E–01	(1.60E+00)[D]
Cl^-	2.15E+01	5.15E+03	8.80E+03	3.68E+04

	Type I (HSH02 0–200m)	Type II (KFM02A 509–516m)	Type III (KSH01A 558–565m)	Type IV (KLX02 1,383–1,392m)
	Fresh water	Groundwater with marine character	Present groundwater at repository level	Brine type water of very high salinity
Br^-	(2.00E–01)[B]	2.20E+01	7.10E+01	5.09E+02
SO_4^{2-}	8.56E+00	5.10E+02	2.21E+02	1.21E+03
Si(tot)	6.56E+00	5.20E+00	4.70E+00	2.60E+00
HCO_3^-	2.52E+02	1.24E+02	1.20E+01	4.20E+01
S^{2-}	(1.00E–02)[B]	5.00E–02	5.00E–02	5.00E–02
pH	8.58	7.1	7.45	6.8

A) No measurements available, data imported from KSH01 #5263.
B) Based on detection limit.
C) Based on the Fe-tot measurement.
D) No measurements available, data imported from KLX02 #2731.

2.3 Transport data

2.3.1 Site investigation data

About 130 rock samples from boreholes KSH01, KSH02 and KSH03 on the Simpevarp peninsula have been selected for the laboratory investigations within the Transport programme. These laboratory measurements are performed in order to obtain site-specific diffusion and sorption parameters for the different rock types in the area. The sample selection was made in accordance with the "Laboratory strategy report"/Widestrand et al. 2003/. It primarily includes major rock types, fractures and deformation zones, but also, to a smaller extent, minor rock types and altered bedrock. Measurements are performed on samples from different depths in the boreholes in order to describe the heterogeneity of the retardation parameters and the possible effects of stress release (an issue addressed in the investigation by /Winberg et al. 2003/). The selection of samples from fractures/deformation zones was mainly controlled by the indications of water flow, as recorded in flow logs.

Through-diffusion experiments and batch sorption experiments are performed at Chalmers University of Technology (CTH) in Gothenburg and at the Royal Institute of Technology (KTH) in Stockholm. Since the experiments are still in progress, the dataset available for use in the transport modelling is rather limited. The "extraction" of data from the on-going measurements is described below, see also /Gustavsson and Gunnarsson, 2005/. Laboratory electrical resistivity measurements have been performed at KTH; the results of the resistivity measurements are interpreted in terms of the so-called "formation factor", which can be related to the diffusivity. Also *in situ* formation factors, based on interpretations of measurements in the Simpevarp boreholes, have been delivered by KTH /Löfgren and Neretnieks, 2005/. Porosity measurements have been performed in connection with the through-diffusion and laboratory resistivity measurements.

The site investigation data available for the S1.2 modelling include data from the water saturation porosity measurements on major rock types, a few preliminary through-diffusion data, and formation factors obtained from laboratory and *in situ* resistivity measurements. In addition, some BET surface area data on the major rock types are presented; BET (Brunauer, Emmet, Teller, see /Brunauer et al. 1938/) is a method for measuring the specific surface area of a solid material by use of gas adsorption. PMMA (polymethylmethaacrylate) porosity measurements, which is an impregnation method for studying the pore system /Byegård et al. 1998; Hellmuth et al. 1993, 1994/, and through-diffusion measurements with helium gas are to be done during winter/spring 2005. Therefore, no results obtained with these methods are presented in this model version.

2.3.2 Application of Äspö HRL data to Simpevarp

The potential for "importing" Äspö HRL data for use within the site descriptive modelling has been further evaluated in the S1.2 modelling. Due to the lack of data for the "Simpevarp rock types", it has been necessary to import transport data to parameterise an initial retardation model. The imported data are from through-diffusion and batch sorption laboratory measurements on the "Äspö rock types", particularly Äspö diorite and fine-grained granite /Byegård et al. 1998; Dershowitz et al. 2003/.

Äspö diorite could be described as a medium-grained and porphyritic quartz monzodiorite/ granodiorite, which contains K-feldspar phenocrysts and has been closely related to Ävrö granite in the Äspö region. The modal composition of the Äspö diorite shows variations from mainly granodiorite to quartz monzodiorite, but granites and tonalities are also found /Byegård et al, 1998; Tullborg, 1995/.

The quartz monzodiorite at the Simpevarp peninsula is defined as equigranular to weakly porphyritic and quartz monzonitic to monzodioritic in its composition. Ävrö granite is described as generally porphyritic, granitic to quartz monzodioritic. Consequently, quartz monzodiorite and Ävrö granite have overlapping compositional ranges, including granitic-granodioritic-quartz monzodioritic-dioritic compositions, as shown in Figure 2-5. Therefore, quartz monzodiorite and Ävrö granite have mainly been distinguished by their different textures and/or grain sizes. The transposition between rock types from the Simpevarp area and the somewhat older nomenclature for "Äspö rock types" is shown in Table 2-5. This table shows that Äspö diorite is considered to be equivalent to the quartz monzodiorite at Simpevarp, mainly because of similarities in their geochemical compositions.

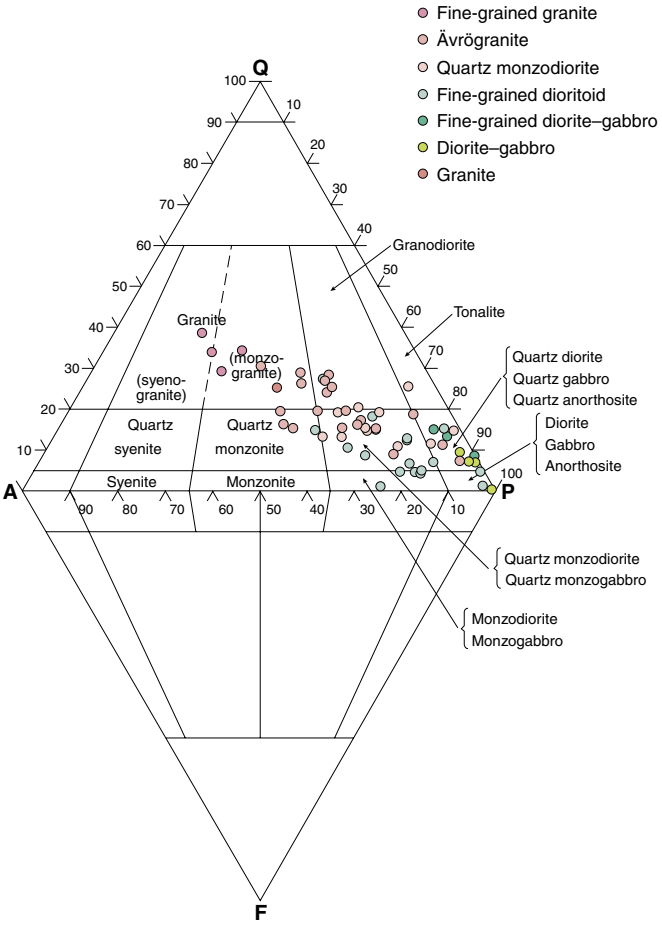

Figure 2-5. *QAPF modal classification of rock types in the Simpevarp subarea. Modal analyses of samples from KSH01A+B and KSH02 are also included /SKB, 2005/.*

Table 2-5. Nomenclature for rock types in the Oskarshamn site investigation (from SKB-internal rock nomenclature memo).

Simpevarp area rock name	Äspö rock name	Descriptive name
Ävrö granite	Småland-Ävrö granite	Granite to quartz monzodiorite, generally porphyritic
Quartz monzodiorite	Äspö diorite, tonalite	Quartz monzonite to monzodiorite, equigranular to weakly porphyritic
Fine-grained dioritoid	Metavolcanite, volcanite	Intermediate magmatic rock
Fine-grained granite	Fine-grained granite	Granite, fine- to medium-grained
Granite	Granite	Granite, medium- to coarse-grained
Fine-granied diorite-gabbro	Greenstone	Mafic rock, fine-grained

In conclusion, Ävrö granite is generally unequigranular and porphyritic in texture, and ranges in composition from granite to quartz monzodiorite with a majority of the samples plotting in the granodiorite/quartz monzodiorite fields /SKB, 2005; Chapter 5/. The porosity interval of the Ävrö granite samples is in better agreement with the data for the Äspö diorite; it is therefore suggested that diffusivity data for the Äspö diorite can be used for the Ävrö granite.

Contrary to the diffusion characteristics, the sorption properties are considered to be more closely related to the mineralogical composition than to the texture of the rock type. For the import of Äspö diorite data to the similar Simpevarp rock types (i.e. Ävrö granite, quartz monzodiorite and fine-grained dioritoid) comparisons of mineralogy is of importance.

Based on the recently performed mineralogical investigation of the different major rock types /SKB, 2005; Figure 5-15/, it can be observed that the mineralogical compositions of Ävrö granite, quartz monzodiorite and fine-grained dioritoid give quite similar values for, e.g. the biotite and the plagioclase contents (12–16% and 46–51%, respectively). Calculations reported by /Dershowitz et al. 2003/ have indicated that > 90% of the cation exchange capacity of the Äspö diorite can be attributed to the biotite and plagioclase contents. For these reasons, it has been decided that sorption coefficients for cation exchange sorbing radionuclides determined using Äspö diorite should be considered valid also for Ävrö granite, quartz monzodiorite and fine-grained dioritoid.

3 Analyses and evaluation of Transport data

In this chapter, the data used (i.e. site-specific data and/or data imported from other works) for establishing the retardation models are described. According to the basic conceptual model for radionuclide retention, see Section 1.2.1, the considered retardation processes can be described as:

A. Adsorption on surfaces of materials present in or at the fracture walls, which are considered to be directly accessible (no significant diffusion needed) during the transport. These fracture surface reactions are considered to be independent of the flow rate and the residence time in the fracture, and can thus be simply described by an equilibrium surface sorption coefficient, K_a (m). The retardation obtained by this process can be described by a retardation factor, R_f, defined as:

   $R_f = 1 + \frac{2K_a}{b}$, where b is the aperture of the fracture.

B. Diffusion into the rock matrix and a potential adsorption on the inner surfaces of the rock material. This process is dependent on the following parameters:
   a. The amount of inner volume (pores) in the rock matrix that is available for diffusion, i.e. the porosity, θ_m (–).
   b. The rate at which the radionuclide diffuses in the rock matrix, i.e. the effective diffusivity, D_e (m^2/s).
   c. The partitioning coefficient describing the distribution of the radionuclide between the inner surfaces of the pores and the water volume of the pores, K_d (m^3/kg).

In the time perspective relevant for storage of nuclear waste, the A process can often be neglected compared to the B process.

3.1 Porosity

3.1.1 Methods

Porosity refers to the volume of the rock that is filled with water and available for diffusion. In the conceptual model used in this work, the micro-scale porosity is considered to be homogeneously distributed in the rock matrix. Studies of the spatial distribution of porosity in the micro scale (PMMA measurements) are planned in the site investigation programme, but have not been performed so far.

The porosity data used in the site descriptive transport modelling have mainly been obtained from measurements done on rock samples aimed for diffusion and sorption studies. The method used for determination (SS-EN 1936) consists of a water saturation of the sample, followed by a drying step. The drying of the samples is done at a temperature of 70°C, which differs from the temperature (105°C) used in the method for porosity measurements in the geology programme of the site investigation. The reason for this is that the samples in the transport programme are designated for other laboratory investigations afterwards. For the interpretation of these laboratory investigations (diffusion and sorption measurements), it is important to avoid the extra chemical and mechanical degradation of the samples that could result from the higher drying temperature.

It should also be emphasized that a measurement of the porosity is also obtained in the through-diffusion measurements (cf Section 3.2). From the fitting of the experimental results to the diffusion model, the "capacity factor" (denoted α) is obtained, which for the non-sorbing tracer HTO should be equivalent to the porosity. However, the main source of porosity data in this work is the water saturation measurements. Capacity factor measurements are used for comparative purposes only.

3.1.2 Site-specific porosity data

The results of the porosity measurements are summarized in Table 3-1, and are also presented on a detailed sample level in Appendix 1. Clearly, the large standard deviations of some of the data in Table 3-1, with sample mean minus σ showing negative values in some cases, indicate that log-normal distributions are more appropriate than, e.g. normal or rectangular distributions for describing the data.

The geological characterisation in binocular microscope shows a great number of small cracks that are 3–15 mm in length and with a width of ≤0.5 mm in both fresh and altered rock samples. These cracks are thus larger than intragranular micro cracks /Ståhle, 2001/, and cut right through mineral grains. Table 3-1 includes results where the samples with cracks have been excluded; comparisons with the complete datasets indicate that the cracks may increase the porosity. Both concerning the porosity and the diffusivity (cf Section 3.2) of the rock samples, the induced stress release during the sampling is suspected to cause overestimation of the measured parameters.

For the diffusivity, corresponding *in situ* measurements are available, which enables an evaluation of the effects of the stress release. Since no *in situ* porosity measurements are available, no direct corresponding analysis can be made of the porosity parameter. However, porosity and diffusivity are parameters generally considered to be closely related to each other. According to this consideration, estimations of the impact of stress release on the porosity measurements could be obtained from the *in situ* diffusivity measurements.

Another possible effect of the sampling of the rock is that the drilling and sawing may induce increased numbers micro-fractures in the samples, which thus may increase the porosity in the rock closest to the edges of the sampled rock. It follows that this effect should be more pronounced in shorter rock samples. The effect of the sample length is illustrated in Table 3-2, which indicates that the measurement method gives an increase in porosity values with shorter sample lengths. This statement is supported by earlier porosity measurements in connection with diffusion experiments /Johansson et al. 1997/. It should be noted, however, that the statistical significance of the data in Table 3-2 is questionable (few samples), which is also the case for some of the results in Table 3-1.

Alteration of the rock is suspected to be a factor that can influence the porosity, as shown in previous investigations /Eliasson, 1993/. In this stage of the laboratory investigations, there is not enough data to quantify an alteration effect on the porosity, but this effect should be considered in forthcoming evaluations of data from the on-going site investigations.

3.1.3 Imported data

Presently, no results of porosity measurements on the altered rock material close to fractures are available. A material considered to represent this material is the altered Äspö diorite, studied by /Byegård et al. 2001/. In their work, an 8 mm thick 2 cm by 2 cm isolated sample of altered Äspö diorite (sampled at Äspö HRL, Feature A intercept with KXTT2, 15.10 m) was exposed to water saturation porosity measurements followed by a diffusion experiment with tritiated water (HTO). The methods used in this work were almost exactly the same as in the method descriptions for the site investigation laboratory experiments; hence, import of data from this work seems motivated. The porosity measurement on the altered Äspö diorite gave a result of 0.33%, which is also included in Table 3-1.

It should also be noted that the porosity values for Ävrö granite and fine-grained dioritoid in the geological S1.2 model /SKB, 2005; Chapter 11/ are higher than those presented in Table 3-1. This could be due to the fact that the results presented by Geology are from outcrops and not from drill cores.

Table 3-1. Porosities (vol-%) of different rock types from the Simpevarp area (number of samples within parenthesis). The values are given as mean value ± 1σ of the experimental dataset (non-log and log_{10} values for each rock type).

Rock type	All rock samples (n)	Rock samples without cracks (n)
Fine-grained dioritoid	0.21 ± 0.21 (87) $10^{(-0.82 \pm 0.38)}$	0.17 ± 0.15 (63) $10^{(-0.90 \pm 0.35)}$
Quartz monzodiorite	0.26 ± 0.31 (23) $10^{(-0.75 \pm 0.35)}$	0.20 ± 0.13 (22) $10^{(-0.80 \pm 0.28)}$
Ävrö granite	0.40 ± 0.13 (19) $10^{(-0.43 \pm 0.19)}$	No samples excluded
Fine-grained granite	0.29 ± 0.23 (17) $10^{(-0.70 \pm 0.34)}$	0.22 ± 0.09 (15) $10^{(-0.73 \pm 0.31)}$
Altered Äspö diorite (data imported from /Byegård et al. 2001/)	0.33 (1)	No samples excluded

Table 3-2. Porosities (vol-%) for rock samples of different lengths (number of samples within parenthesis). The values are given as mean value ± 1σ of the experimental dataset.

	Samples ≤ 1 cm (n)	Samples 3 cm (n)	Samples 5 cm (n)
Fine-grained dioritoid	0.32 ± 0.18 (12)		0.17 ± 0.16 (6)
Ävrö granite	0.52 ± 0.6 (6)	0.34 ± 0.12 (11)	

3.2 Diffusion

3.2.1 Methods and parameters

In this work, the term diffusion refers to the process in which a tracer can diffuse from the fracture water volume into the micro fractures of the rock matrix. Thereby, an interaction can occur in which the inner surfaces of the rock matrix can be available for sorption, and the tracers can be significantly retarded in their transport. The present work addresses diffusion processes in the aqueous phase only; potential diffusive mobility in the adsorbed state (so-called surface diffusion /Ohlsson and Neretnieks, 1997/) is not considered.

Two main methods for the determination of the diffusivity of the rock materials are used within the site investigations /Widestrand et al. 2003/:

- Through-diffusion measurements; a method where the effective diffusivity, D_e (m^2/s), is determined by studying the diffusion rate of tritiated water (HTO) through a rock sample (HTO is used in the site investigations; the method can be applied also with other tracer solutions).
- Resistivity measurements; a method where the information on the diffusivity is obtained from the resistivity of electrolyte-saturated rock samples.

The diffusion process is quantified in terms of the formation factor, F_m (–). This parameter quantifies the reduced diffusion rate obtained in the rock material relative to the diffusion rate in pure electrolyte. It is thus calculated from the results of the through-diffusion studies, as:

$$F_m = \frac{D_e}{D_w} \tag{3.1}$$

where D_w (m^2/s) is the diffusivity of tritiated water in pure water, i.e. 2.13×10^{-9} m^2/s /Li and Gregory, 1974/.

For the resistivity measurements, F_m is the parameter produced by the method, i.e. the ratio of the resistivity of a given electrolyte to the resistivity of the rock sample with the pores saturated with the same electrolyte.

The resistivity can be measured both in laboratory experiments (where the rock samples are saturated with 1 M NaCl) and in borehole *in situ* experiments. For obvious reasons, no saturation of the rock matrix with a known electrolyte can be done in *in situ* experiments. In this case, the composition of the pore liquid must be estimated based on hydrogeochemical sampling and analysis, commonly assuming the same composition in the matrix as in the groundwater in neighbouring fractures. A further complication is that a lower salinity than 1 M NaCl, which thus likely could be present in the pores in *in situ* rock, according to /Ohlsson and Neretnieks, 1997/ attributes a significant part of the conductivity to the surface ion mobility.

3.2.2 Through-diffusion studies

Site-specific data

Site specific rock materials from the Simpevarp site have been sampled and used in through-diffusion measurements in accordance with the SKB method description (SKB internal document). These measurements are time consuming, and steady state conditions

(necessary for final evaluation) have not been obtained in most samples. However, for the parameterisation of the S1.2 retardation model, a selection of results from on-going through-diffusion experiments has been done. Based on these data, preliminary diffusivities were evaluated.

The diffusivity is determined by studying the diffusion of tritiated water (HTO) through a slice of rock. A slice of water-saturated rock is mounted in a diffusion cell, where the start cell is filled with water spiked with HTO tracer and the other side is filled with non-spiked water. The rate of diffusion is evaluated from the rate of the in-growth of the HTO tracer in the originally non-spiked water volume. The effective diffusivity, D_e (m^2/s), and the rock capacity factor, α (–), are calculated by fitting the model equation:

$$C_r = \frac{C_2 V_2}{C_1 A l} = \frac{D_e t}{l^2} - \frac{\alpha}{6} - \frac{2\alpha}{\pi^2}\sum_{n=1}^{\infty}\frac{(-1)^n}{n^2}\exp\left\{-\frac{D_e n^2 \pi^2 t}{l^2 \alpha}\right\} \quad (3.2)$$

where C_2 (Bq/m^3) is the accumulated tracer concentration in the target cell at the time t (s), V_2 (m^3) is the volume of the target cell, C_1 (Bq/m^3) is the tracer concentration in the start cell, A (m^2) is the geometric surface area of the rock sample, and l (m) is the length of the rock sample. The results of the preliminary evaluation of the on-going through-diffusion experiments are presented in Table 3-3.

Table 3-3. Preliminary results from through-diffusion experiments on rock samples from KSH01A and KSH02. The effective diffusivity, D_e, and the rock capacity factor, α, were obtained from least-square fits to the experimental data.

Rock type	SKB ID	Sample thickness (mm)	D_e (m^2/s)	α (–)
Ävrö granite	KSH01A 891.66–891.67	5	1.26E–12	1.31E–02
	KSH01A 891.77–891.78	5	1.01E–12	1.52E–02
	KSH01A 891.88–891.89	5	1.11E–12	1.00E–02
Fine-grained dioritoid	KSH01A 940.80–940.85	30	4.28E–13	8.85E–03
	KSH02 474.46–474.47	5	7.40E–14	4.67E–03
	KSH02 474.47–474.48	10	4.96E–14	5.84E–03

Imported Äspö HRL data

Since no site specific through-diffusion measurements are available for Simpevarp rock types other than Ävrö granite and fine-grained dioritoid, the possibilities of importing data from Äspö HRL investigations were evaluated. Based on the reasoning in Section 2.3.2, import of Äspö diorite data for the Ävrö granite and of data for fine-grained granite can be justified. However, since site specific diffusivity data are available for Ävrö granite, no need of import of Äspö diorite data seems motivated. For the remaining rock types, i.e. quartz monzodiorite, granite and fine-grained diorite-gabbro, no data are available. Therefore, the through-diffusion characteristics of these rock types must be considered pending in S1.2 description.

For the import of fine-grained granite data from the investigation presented by /Byegård et al. 1998/, see Table 3-4, diffusivities have been selected only from samples where the evaluated porosities overlap with the observed corresponding porosity interval in the site investigation, cf Figure 3-1.

As mentioned in the previous section, porosity and diffusion parameters of altered Äspö diorite are imported from /Byegård et al. 2001/. In their work, several different evaluation methods were applied to the diffusion results, addressing, e.g. multi-rate diffusion. Of these evaluation methods, the method concluded to be most similar to that described in the site investigation method description is the one where the water saturation porosity results are used and only a single diffusion rate is varied in order to fit the experimental results. This analysis gave a diffusivity of 1.6E–13 m^2/s, corresponding to a formation factor of ~ 8E–5. Addressing the uncertainty in this single measurement is difficult; a proper quantification cannot be obtained until more data have been obtained. A summary of the through-diffusion results is given in Table 3-6, where also comparisons are made to the results obtained by the electrical resistivity measurements.

Table 3-4. Porosities, effective diffusivities and formation factors for individual samples of fine-grained granite, FGG /Byegård et al. 1998/. The intervals express the estimated measurement uncertainty for a single sample, based on the fitting of Equation (3.2) to the through-diffusion data.

Sample ID	Porosity θ_m (%)	Diffusivity D_e (m^2/s)	Formation factor F_m (–)
FGG1	0.47 ± 0.03	1.0E–13 ± 1.0E–15	4.7E–05 ± 3.0E–08
FGG2	0.44 ± 0.03	7.5E–13 ± 1.2E–15	3.5E–05 ± 3.8E–08
FGG6	0.70 ± 0.01	6.2E–13 ± 1.0E–15	2.9E–05 ± 6.7E–09
FGG8	0.34 ± 0.01	1.2E–13 ± 3.0E–15	5.6E–05 ± 4.1E–08
FGG9	0.24 ± 0.05	6.2E–13 ± 3.5E–15	2.9E–05 ± 3.4E–07
FGG14	0.86 ± 0.26	4.0E–13 ± 8.0E–15	1.9E–04 ± 1.1E–06
FGG16	0.53 ± 0.08	2.2E–13 ± 7.0E–15	1.0E–04 ± 5.0E–07
FGG18	0.12 ± 0.03	6.8E–13 ± 1.2E–15	3.2E–05 ± 1.4E–07
FGG20	0.089 ± 0.018	4.3E–13 ± 2.1E–15	2.0E–05 ± 2.0E–07
FGG22	0.41 ± 0.13	1.8E–13 ± 3.0E–15	8.5E–05 ± 4.5E–07
FGG24	0.11 ± 0.03	5.1E–13 ± 2.5E–15	2.4E–05 ± 3.2E–07
FGG26	0.49 ± 0.06	7.2E–13 ± 1.2E–15	3.4E–05 ± 6.9E–08

Table 3-5. Formation factors imported for fine-grained granite from diffusion investigation of the Äspö rock material /Byegård et al. 1998/.

Rock type	Measured porosity* and number of measured samples in the site investigation program (%)	Number of samples selected from TR-98-18 (total number)	Porosity (%) based on the selected samples	Formation factor (F_m) based on the selected samples
Fine-grained granite	0.22 ± 0.09 (15)	4 (12)	0.22 ± 0.14	(4 ± 3)E–5

* As described in connection with Table 3-1, data originating from samples with visible cracks are excluded.

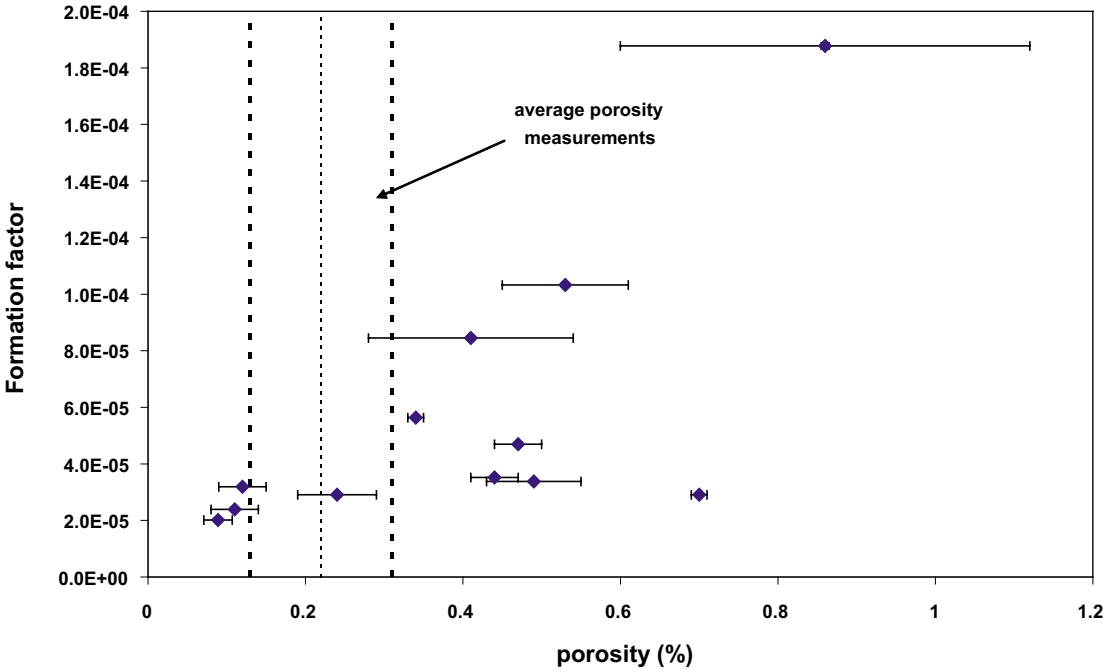

Figure 3-1. *Formation factor versus the porosity (determined from the capacity factor, α, in through-diffusion experiments /Byegård et al. 1998/) for fine-grained granite samples from the Äspö HRL. The intervals obtained for the porosity measurements (average ± 1 standard deviation) on fine-grained granite samples from the Simpevarp site have been marked by vertical lines in the figure.*

3.2.3 Electrical resistivity

A summary of the results of the electrical resistivity measurements reported by /Löfgren and Neretnieks, 2005/ is provided in Table 3-6; the individual measurement results can be found in Appendix 2. In Table 3-6, the results are expressed in terms of both non-log and $\log_{10}$ values. Similar to the porosity data discussed above, standard deviations are in many cases of the same order as, or even larger than, the mean values. Some general observations made in the electrical resistivity data are presented in the following.

Laboratory resistivity versus porosity

As expected, a tendency of increased formation factor with increasing porosity can be observed in the results (Figure 3-2). However, it is obvious that the data cannot be described by a normal distribution, neither for the formation factor nor for the porosity. A presentation of the data in log-log scale (Figure 3-3) indicates that the porosity and diffusivity characteristics should instead be described using log-normal distributions. Distribution plots for formation factors and porosity data for samples consisting of fine-grained dioritoid (Figures 3-4 and 3-5) indicates a reasonably log-normal distribution of the porosity, whereas the formation factor shows larger deviations from a log-normal distribution.

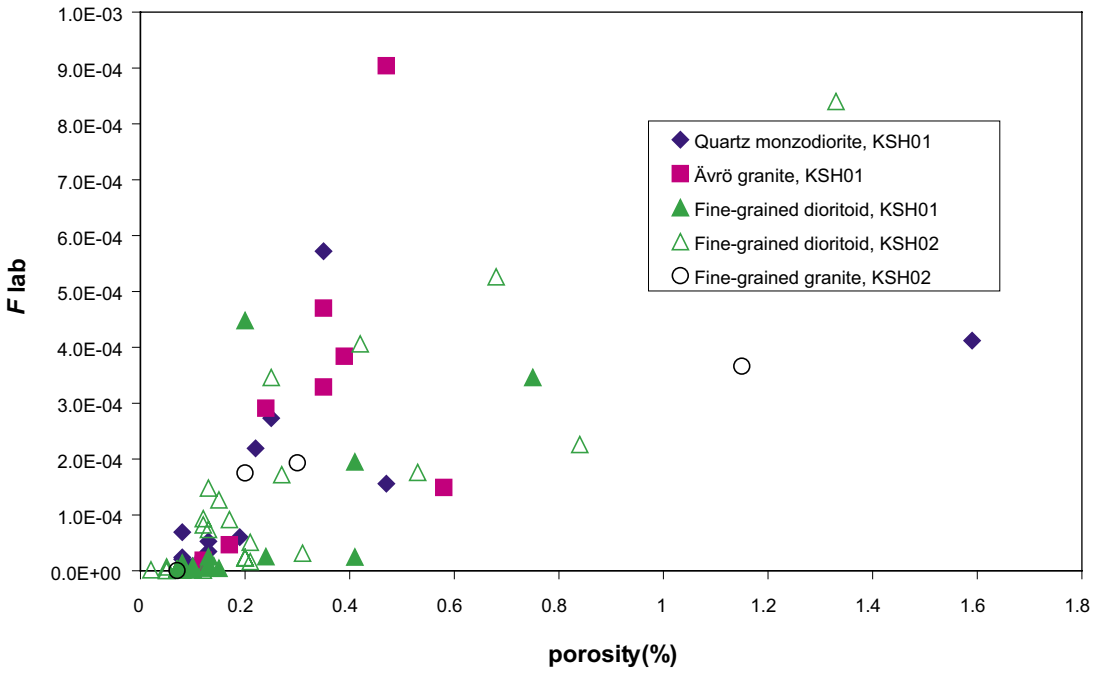

Figure 3-2. *Formation factor versus the porosity, using formation factors determined in electrical resistivity measurements in the laboratory /Löfgren and Neretnieks, 2005/. The porosities were measured using the water saturation method (SS-EN 1936).*

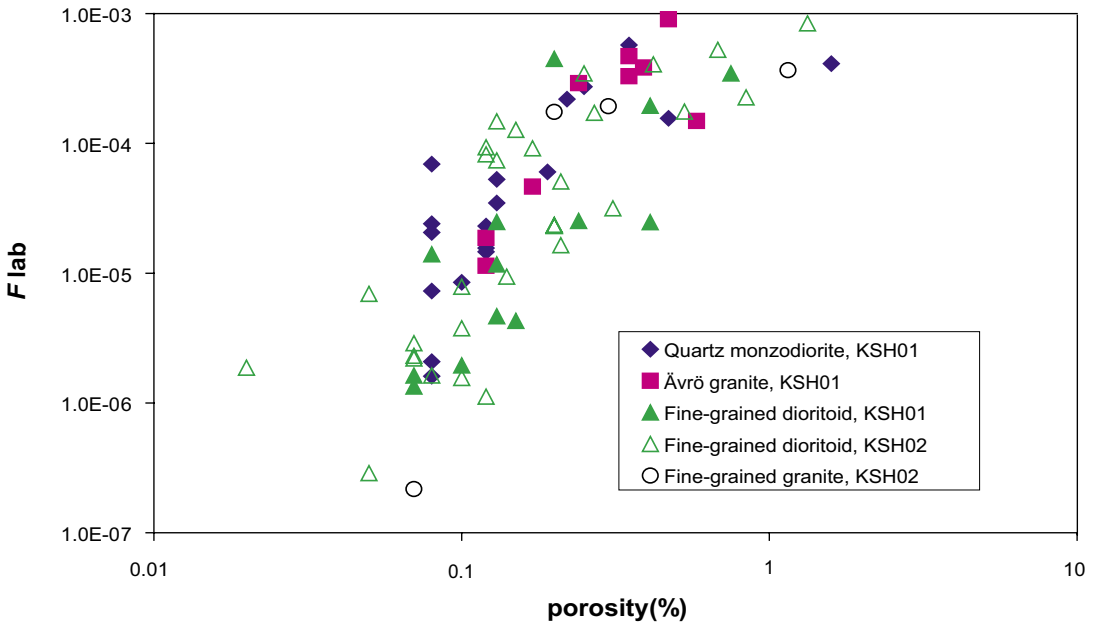

Figure 3-3. *Formation factor versus the porosity (in log-log scale), using formation factors determined from electrical resistivity measurements in the laboratory /Löfgren and Neretnieks, 2005/. The porosities were measured using the water saturation method (SS-EN 1936).*

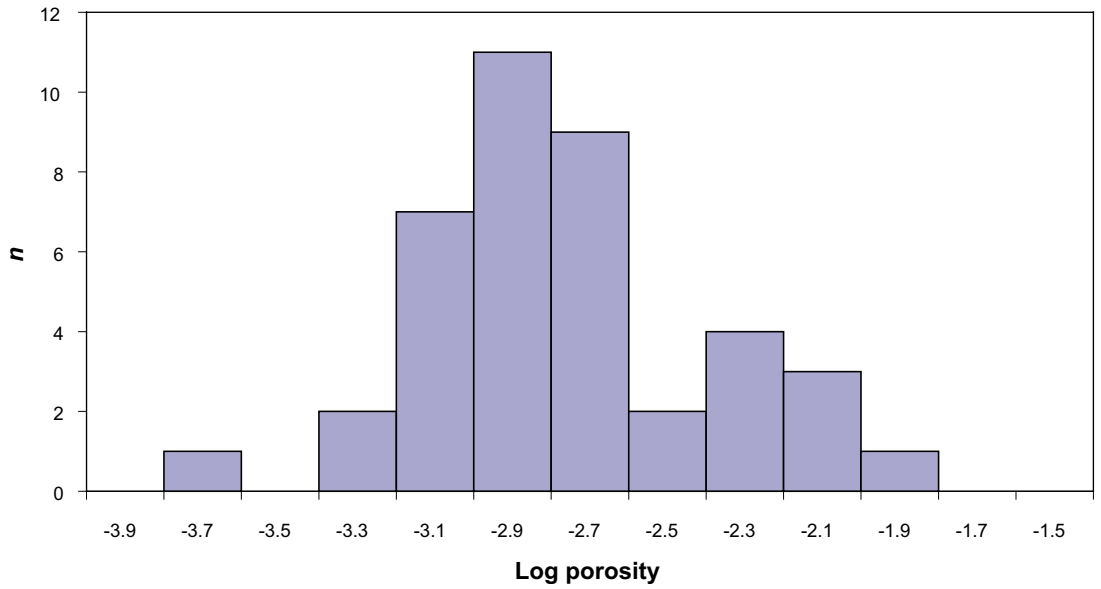

Figure 3-4. *Distribution of porosity on log-scale for the fine-grained dioritoid samples.*

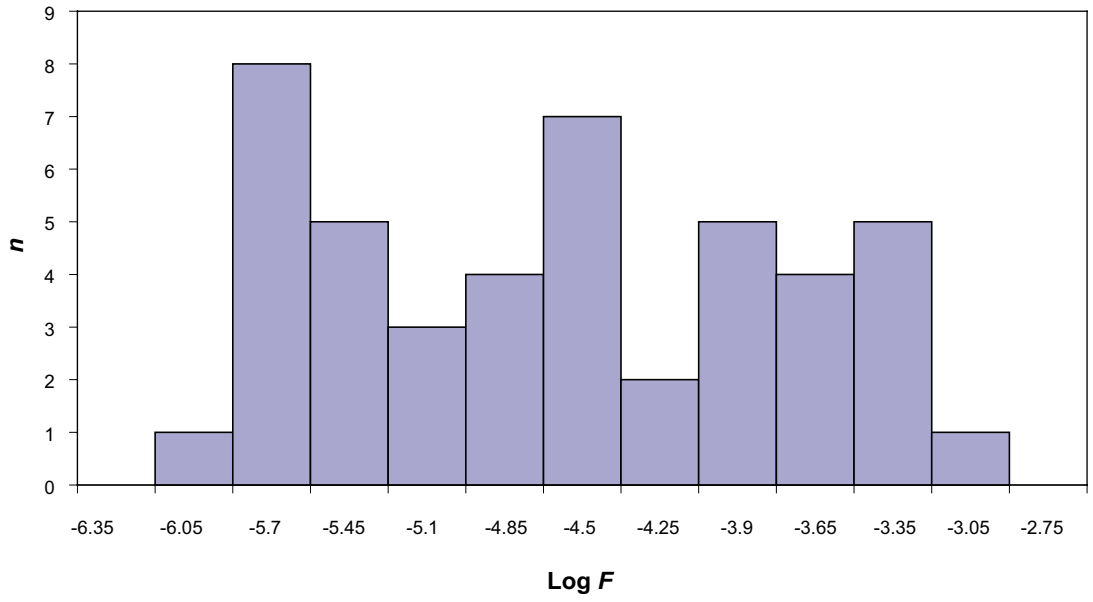

Figure 3-5. *Distribution of the formation factor on log-scale for the fine-grained dioritoid samples.*

Formation factor versus borehole length

Data are presented both for the laboratory measurements (Figure 3-6) and for the *in situ* measurements (Figure 3-7). A comparison indicates a much larger spread in the data for the laboratory samples than in the *in situ* measurement data. As discussed by /Löfgren and Neretnieks, 2005/, this difference can, at least partly, be explained by a truncation of low formation factor values in the *in situ* measurements, caused by the limited measurement range of the equipment used. Specifically, Figure 3-7 shows that the formation factor distribution from KSH01A is truncated at approximately 1E–5, and that from KSH02 at a slightly lower level.

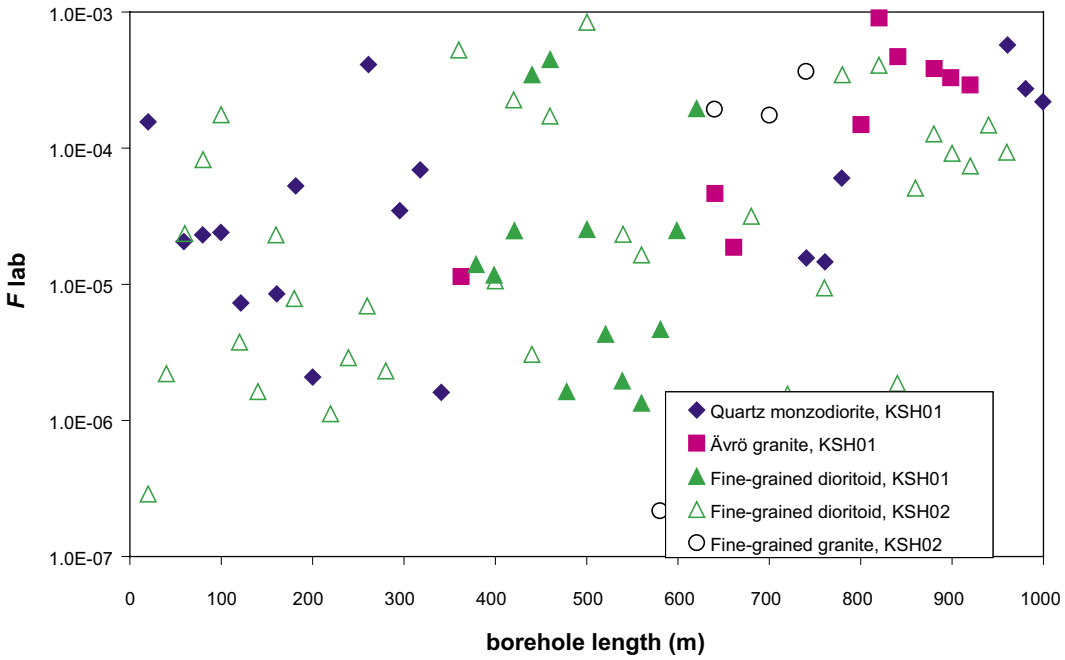

Figure 3-6. *Formation factors measured with electrical resistivity in the laboratory versus the borehole length, i.e. the position in the borehole where the sample was taken.*

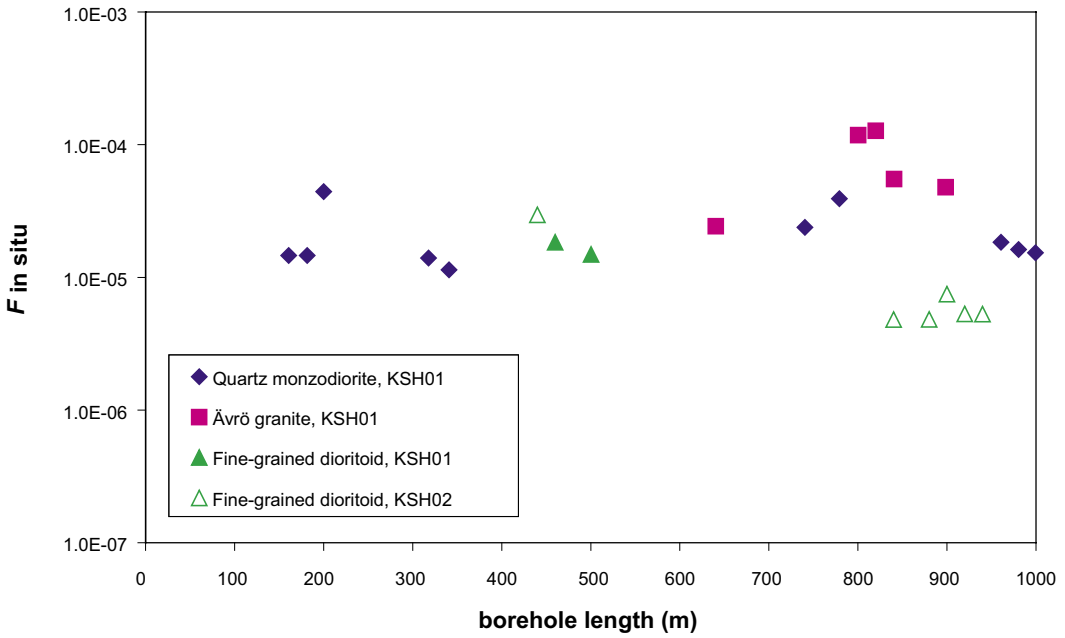

Figure 3-7. *Formation factors measured with electrical resistivity in situ versus the borehole length.*

Due to the large scatter in the dataset, it is difficult to identify any particular trend in the laboratory data. For example, no clear trend can be observed that indicates a significant increase in diffusivity in samples from larger depths, which, if present, could indicate an increased effect of stress release on these samples (cf Figure 3-8). It is also difficult to observe such a trend in the representation of the porosity versus the sample depth for the laboratory samples (Figure 3-9). Possibly, an increase could be observed in formation factor and porosity values for Ävrö granite and quartz monzodiorite for samples from borehole lengths larger than approximately 800 m.

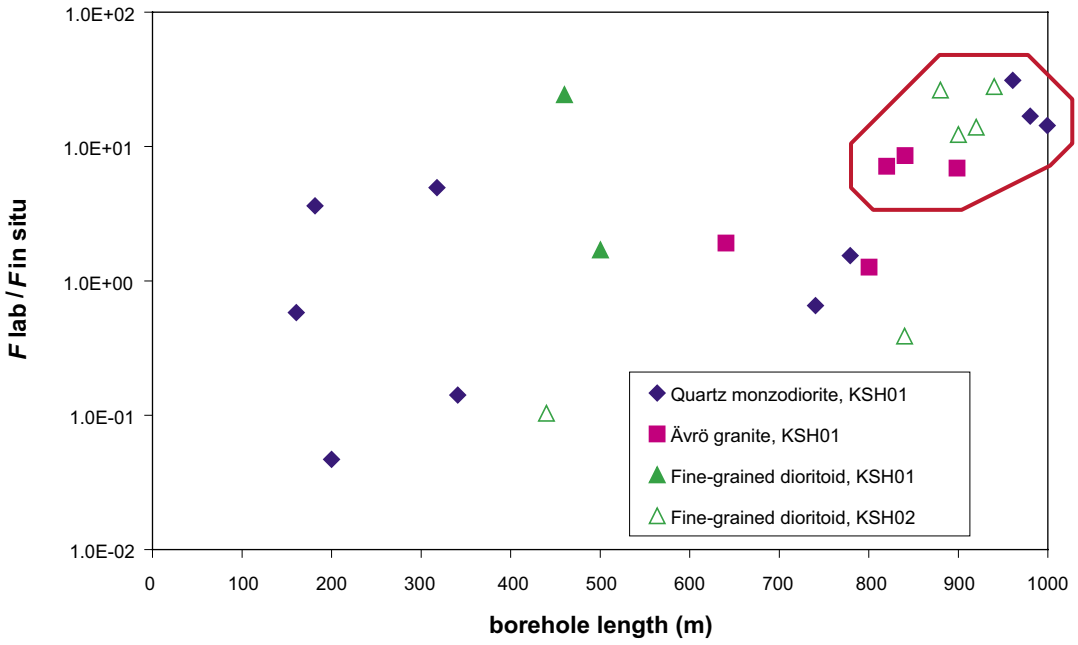

Figure 3-8. *Ratio of the formation factors measured in the laboratory and in situ with electrical resistivity versus the borehole length. The marked area in the upper right part of the figure corresponds to a number of samples at large depth that are suspected to have undergone a marked stress release, i.e. the* F_{lab} *is significantly larger than the corresponding* $F_{in\ situ}$.

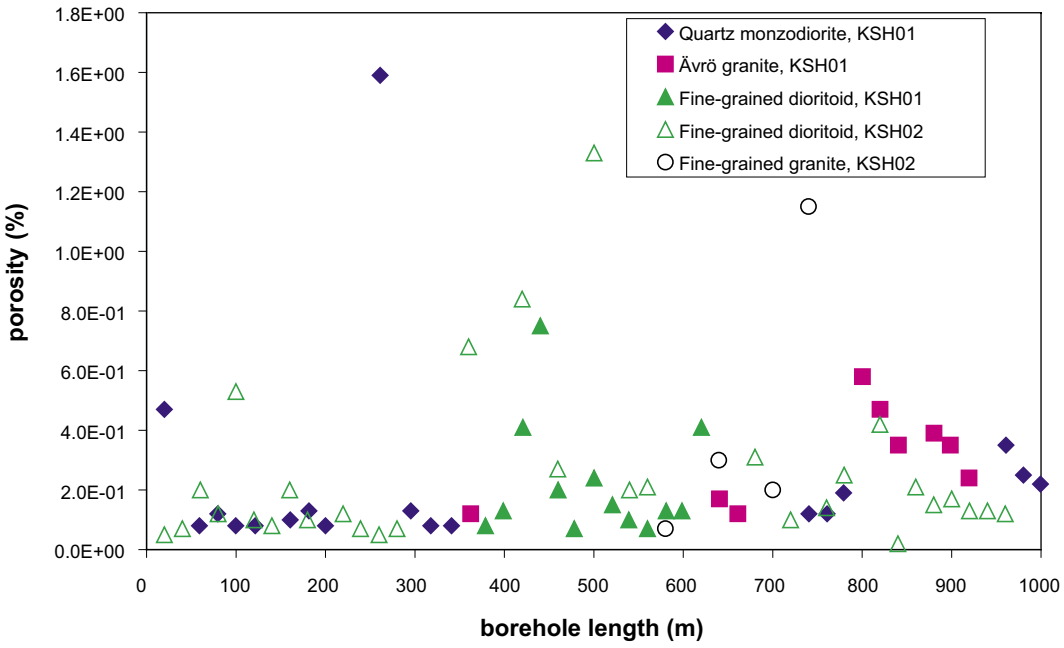

Figure 3-9. *Porosity, measured in the laboratory using the water saturation method, versus the borehole length.*

This possible effect of stress release is indicated by the increased $F_{lab}/F_{in\ situ}$-values within the marked area in Figure 3-8. A regression line showing increasing $F_{lab}/F_{in\ situ}$-values with depth could probably be fitted to the data. However, the deviations from such a trend line would be large, and the quantification of the trend uncertain. Therefore, the main observation made at this point is that data from depths larger than 800 m could be taken as indications of stress release effects, which are to be further investigated when more data is at hand.

Table 3-6. Summary of formation factors for the Simpevarp rock types. The values are given as mean values ± 1σ of the considered datasets (non-log and log_{10} values).

Method	Fine-grained dioritoid	Quartz monzodiorite	Ävrö granite	Fine-grained granite	Altered Äspö diorite
HTO through-diffusion	(9 ± 10)E–5	Pending	(5.3 ± 0.6)E–4	(4 ± 3*)E–5	(8 ± 4)E–5
Electrical resistivity, lab	(1.0 ± 1.7)E–4 $10^{(-4.69 \pm 0.89)}$	(1.1 ± 1.6)E–4 $10^{(-4.45 \pm 0.73)}$	(2.9 ± 2.9)E–4 $10^{(-3.85 \pm 0.66)}$	Pending Pending	Pending Pending
Electrical resistivity, *in situ*	(1.1 ± 0.9)E–5 $10^{(-5.05 \pm 0.31)}$	(2.1 ± 1.1)E–5 $10^{(-4.72 \pm 0.20)}$	(7.4 ± 4.5)E–5 $10^{(-4.20 \pm 0.30)}$	Pending Pending	Pending Pending

* Error in /SKB, 2005; Table 10-3/: This is the correct value.

3.3 Sorption

3.3.1 BET surface area

Since the adsorption of radionuclides is taking place on the surfaces of the rock material, the quantification of available surface areas is an important estimation of the sorption capacity of the rock material. For example, different ferric oxides have significant surface areas and have been shown to be highly adsorbing minerals for cations that adsorb with surface complexation, see, e.g. /Jakobsson, 1999/. Furthermore, presence of clay minerals (as a group identified as a significant potential sink for Cs^+) will also cause increased surface areas in the measurements on rock samples.

Although at this stage no method is available for establishing a quantitative relationship between specific surface areas and sorption parameters, results of BET surface area measurements /Brunauer et al. 1938/ are included in the retardation model as qualitative data important for the understanding of the sorption processes. BET measurements have been performed on site-specific materials according to the ISO 9277 standard method. The results of the measurements on the Simpevarp site rock types are given in Table 3-7.

Table 3-7. Measured BET surface area for the fractions 0.045–0.090 mm and 1–2 mm presented together with the results of an extrapolation of the results in order to obtain an inner surface area (concept equivalent to the concept in the K_d extrapolation, cf Equation 3.3).

Rock Type	BET surface area 0.045–0.090 mm (m^2/g)	BET surface area 1–2 mm (m^2/g)	Extrapolated inner BET surface area (m^2/g)
Fine-grained dioritoid	0.57	0.048	0.036
Ävrö granite	0.32	0.041	0.034
Quartz monzodiorite	0.33	0.042	0.035
Fine-grained granite	0.34	0.075	0.069

3.3.2 Sorption data

The process "sorption" is here defined as the adsorptive interaction of radionuclides with the surfaces of the rock material. In the somewhat simplified approach taken in this work, sorption is considered to be:

- Linear (i.e. no concentration effect on the sorption).
- Fast and reversible compared to the considered time perspective (no chemical kinetic effects are addressed for the sorption processes).

The concept used for the sorption processes is the same as described in the "laboratory strategy report" /Widestrand et al. 2003/. This means that the source of sorption data will be batch laboratory experiment performed using crushed and sieved rock material. The results from the measured distribution of tracer between the rock and water phase will be interpreted as:

- Adsorption of the tracers on the outer surfaces of the rock material, determined by the surface sorption parameter, K_a (m).
- Adsorption of the tracers on the inner surfaces of the rock material, determined by the volumetric sorption parameter, K_d (m^3/kg).

In the considered transport concept, the K_a parameter is used only to estimate the minor part of tracer retention that takes place via the sorption on the fracture walls, and is thus of less importance. The major part of the retention is caused by the diffusion of the radionuclides into the rock matrix and the subsequent sorption on the inner surfaces of the rock material.

The evaluation of the batch sorption experimental results to sorption parameters is done according to:

$$R_d = K_d + \frac{6K_a}{d_p \rho} \qquad (3.3)$$

where R_d (m^3/kg) is the measured tracer distribution between solid and liquid phases, d_p (m) is the average particle diameter, and ρ (kg/m^3) is the rock density. A graph of R_d versus $1/d_p$ gives an intercept corresponding to the K_d value, and a slope corresponding to $6K_a/\rho$. This concept of evaluation implies the following assumptions:

- Perfect spherical form of the crushed rock particles.
- The size distributions within each particle diameter interval can be represented by the mean of that interval.

Since there is no established method available for the validation of these assumptions, uncertainty in the resulting sorption has to be acknowledged, although this uncertainty can not be quantified.

Import of Äspö HRL sorption data to the retardation model

The present lack of measured site-specific sorption data from the Simpevarp area implies a need for investigating the possibility of importing Äspö HRL sorption data to this retardation model. A large amount of sorption data is available from the TRUE experimental programme /Byegård et al. 1998/ where sorption investigations were performed using samples of Äspö diorite and fine-grained granite.

In the site description version 1.1, it was recommended to import sorption data according to:

- Data from the Äspö rock type "fine-grained granite" to Simpevarp "fine-grained granite".
- Data from the Äspö rock type "Äspö diorite" to Simpevarp "quartz monzodiorite".

Based on the recently performed mineralogical investigation of the different major rock types, cf Section 2.2.2, it has been concluded that sorption data determined for Äspö diorite should be valid for the Simpevarp rock types Ävrö granite, quartz monzodiorite and fine-grained dioritoid. The results of the BET surface measurements, cf Table 3-7, also indicate a similarity between these three rock types from a sorption perspective. The import of data made in the site description version 1.1 is therefore applied also in this site description; however, with the extension that the Äspö diorite data are considered applicable also to Ävrö granite and fine-grained dioritoid.

The water used in the Äspö HRL experiments had a composition that makes the results applicable for groundwater composition III in Table 2-4. For the other given groundwater compositions, there are no experimental results that can be imported. It should at this stage be emphasized that the similarity described above is based on the chemical and mineralogical compositions, which implies that it can be applied to the sorption part of the retention characteristics only. The textures and grain sizes of these three rock types are quite different, which means that a difference in the porosity/diffusivity parameters can be expected.

The experimental results of the Äspö diorite and fine-grained granite investigations /Byegård et al. 1998/ are given in Figures 3-10 and 3-11 for strontium (Sr) and caesium (Cs), respectively. The results of the evaluation, performed according to the method described above, are summarised in Table 3-8. It can be noted that the K_d-values for altered rock are lower than those for non-altered rock. A reasonable explanation for this difference, supported by observations in /Byegård et al. 1998/, is that it is related to differences in the biotite contents of the materials.

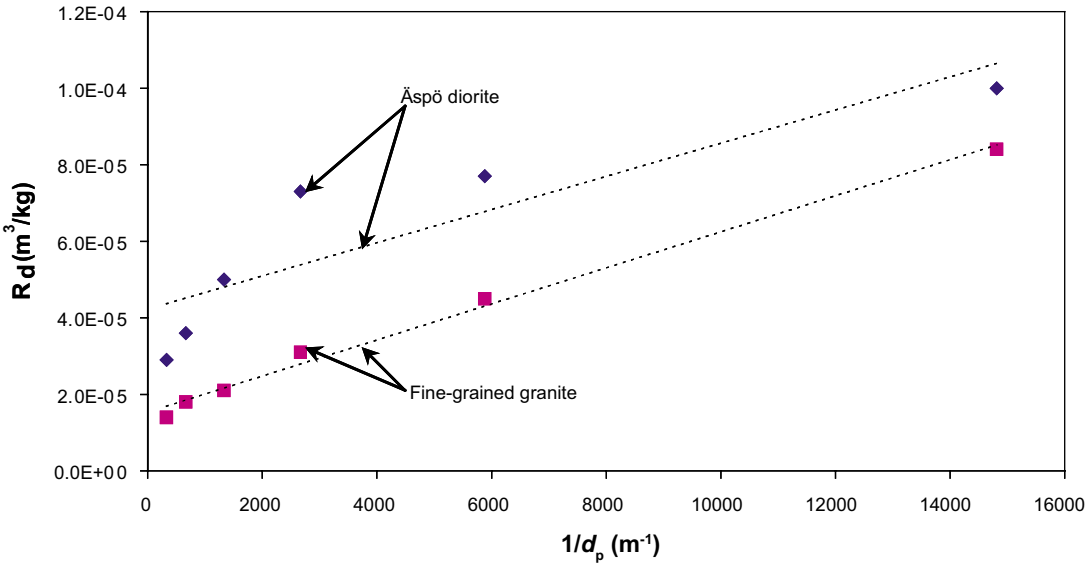

Figure 3-10. *Sorption data for Sr in contact with Äspö diorite and fine-grained granite /Byegård et al. 1998/. Both datasets refer to sorption data determined using a 14 days contact time.*

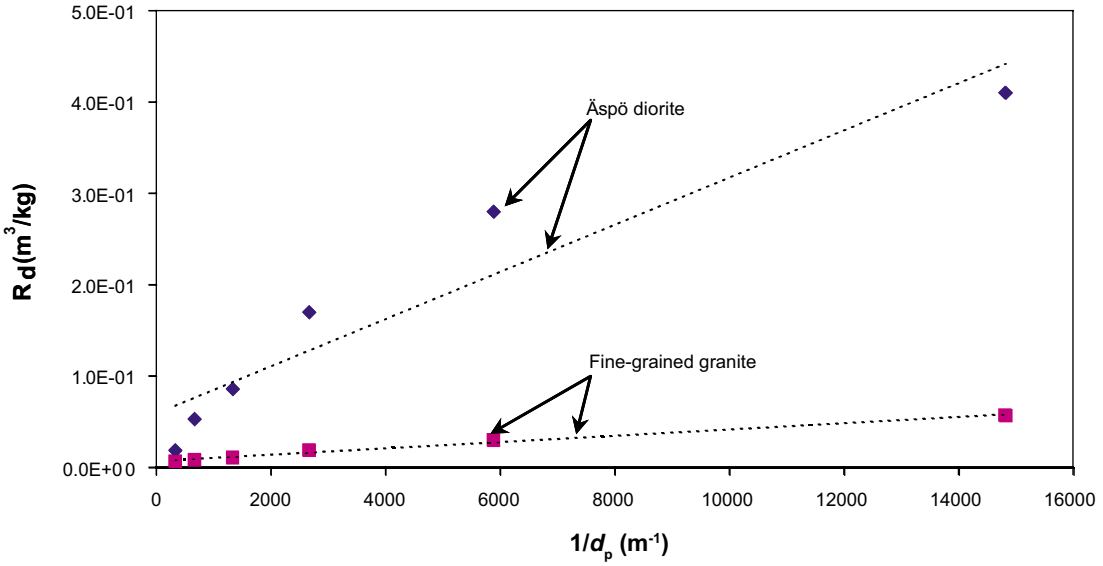

Figure 3-11. *Sorption data for Cs in contact with Äspö diorite and fine-grained granite /Byegård et al. 1998/. The datasets refer to sorption data determined using a 14 days contact time for the fine-grained granite and a 36 days contact time for the Äspö diorite.*

For the transport models, an essential part of the transport has been considered to take place in fractures in altered major rock types (i.e. altered fine-grained dioritoid, quartz monzodiorite and Ävrö granite). The altered Äspö diorite from KXTT2 in the Äspö Hard Rock Laboratory /Byegård et al. 1998/ has been selected as a representative for this rock type. However, a drawback of this dataset is that the published K_d-value was not subject to an evaluation according to Equation 3.3; instead, the distribution coefficient for the size fraction 1–2 mm was chosen as K_d-value.

In order to obtain consistency with the other sorption coefficients used, the following equation was used:

$$K_{d(alt)} = \frac{R_{d(1-2mm)alt}}{R_{d(1-2mm)ÄD}} \cdot K_{d(ÄD)} \qquad (3.4)$$

where $R_{d(1-2mm)}$ is the measured tracer distribution ratio in the 1–2 mm fractions of Äspö diorite (ÄD) and altered Äspö diorite (alt), respectively. $K_{d(ÄD)}$ is the value obtained in the extrapolation of data from all size fraction according to Equation 3.3.

An equivalent calculation has been done in order to obtain the K_a for the altered material, as follows:

$$K_{a(alt)} = \frac{R_{d(1-2mm)alt}}{R_{d(1-2mm)ÄD}} \cdot K_{a(ÄD)} \qquad (3.5)$$

The uncertainties in these calculated values have been set to the same percentage as for the uncertainties obtained for the extrapolated Äspö diorite sorption coefficients.

Table 3-8. Sorption coefficients imported and selected for the Simpevarp 1.2 site description according to the process described above.

Rock type	Sr		Cs	
	K_d (m^3/kg)	K_a (m)	K_d (m^3/kg)	K_a (m)
Non-altered Ävrö granite Quartz monzodiorite Fine-grained dioritoid	(4.2 ± 0.8)E–5	(2.0 ± 0.5)E–6	0.06 ± 0.03	0.012 ± 0.002
Altered Ävrö granite Quartz monzodiorite Fine-grained dioritoid	(1.2 ± 0.2)E–5	(6 ± 1)E–7	0.013 ± 0.006	0.0020 ± 0.0004
Non-altered Fine-grained granite	(1.5 ± 0.1)E–5	(2.12 ± 0.08)E–6	0.007 ± 0.001	0.00155 ± 0.00008

4 Development of retardation model

In accordance with the concept proposed by /Widestrand et al. 2003/, the retardation model should consist of tables in which the geological description and the selected transport parameters for each unit (rock mass or fracture/deformation zone) where retardation of radionuclides can take place are given.

4.1 Methodology

The developed retardation model consists of two parts, one for the major rock types, i.e. for the dominant rock types within the rock domains, and one for the fractures and deformation zones. In the first part, the retention characteristics of the major rock types, i.e. rock matrix interaction parameters, are described. The second part provides a description of the retardation in the water-conducting fractures and deformation zones.

This section lists the parameters presented in the different parts of the model and gives the motivations for the data selections that were made.

4.1.1 Major rock types

According to the retention concept applied in the present work (cf Section 1.2 and Chapter 3), the retardation of radionuclides in the rock matrix can be described using the following parameters:

- Rock matrix porosity, θ_m (–): The results from the water saturation porosity measurements on site-specific rock materials have been selected in this work (cf Table 3-1). A log-normal distribution has been considered to describe the system somewhat better than a normal distribution (although not perfectly), and has therefore been selected for the representation.
- Rock matrix formation factor, F_m (–): This parameter is used to multiply literature values of the radionuclide-specific free diffusivities in water (D_w (m^2/s); tabulated, e.g. by /Ohlsson and Neretnieks, 1997/) to obtain the effective diffusivities, D_e (m^2/s), for the different radionuclides. Since the results of the laboratory electrical resistivity measurements are based on a larger number of samples and have been found not to deviate significantly from the through-diffusion results, they have been selected for the retardation model (cf Table 3-6). For consistency with the closely related porosity parameter, a log-normal distribution has been selected also for the formation factor representation.
- Rock matrix sorption coefficient, K_d (m^3/kg): All available data (all from Äspö HRL investigations, cf Section 3.3.2) are imported for use in the retardation model, according to the description provided in Table 3-8. Site-specific data on the BET surface areas of the different rock types are given as supporting data, see Table 3-7.

4.1.2 Fractures and deformation zones

The present retention concept proposed by /Widestrand et al. 2003/ shall produce retardation models for the identified fracture and deformation zone types by describing and quantifying the retardation properties of the different layers of geological materials present in and in the immediate vicinity of the fractures/deformation zones. The geological materials in the fractures and deformation zones could consist of, e.g. fault gouge, fracture coating, mylonite and altered wall rock. In the retardation modelling, attempts will be made to give the following parameters for the different layers:

- thickness,
- porosity,
- formation factor (to be used in calculations of the diffusivities of the different radionuclides),
- sorption parameters, i.e. surface distribution coefficients, K_a (m), and/or volumetric distribution coefficients, K_d (m^3/kg),
- mineral contents and, if possible, grain sizes.

In addition, the following data on each particular fracture type will be given:

- abundance (percentage) of the fracture type, i.e. a quantification of how large portion of the entire fracture class the given description is valid for,
- transmissivity interval observed for this particular fracture or deformation zone type,
- preferential direction (if any).

In the S1.2 site description, an identification and quantitative description of different fracture types is presented, whereas deformation zone types cannot be identified due to the limited data available. The limited amount of data also implies that some parameter values are missing in the tables describing the identified fracture types.

4.2 Retardation model

4.2.1 Major rock types

The geological model is based on rock domains, whereas the sampling for the transport programme is based on rock types and mainly focused on the three major rock types (Ävrö granite, quartz monzodiorite and fine-grained dioritoid). The samples represent both fresh and altered samples of these rock types. Also minor rock types have been sampled, but no data on these are available at present. The potentially greater importance of the fine-grained granite for transport, indicated by observations of its percentage of open fractures and deviating transport properties at Äspö HRL /Mazurek et al. 1997; Landström and Tullborg, 1993/ and also observed as, e.g. deviations in hydraulic properties, has not been addressed in the present work.

As discussed in previous chapters, large parts of the rock are hydrothermally altered, which is expected to affect the transport properties. This alteration occurs in all three major rock types, but based on observations in boreholes KSH01A, KSH02, KSH03A and KAV01 to less extent in the Ävrö granite than in the two other major rock types.

Table 4-1 present the selected transport parameters for the fresh and altered major rock types. The percentages quantify the portions of the rock types that are altered; they are estimated from data in the S1.2 geological description /SKB, 2005; Chapter 5/, where only the classes referred to as weak, medium and strong alteration have been considered. The parameterisation of the major rock types can then be used to parameterise the different rock domains. Three different domains constitute the rock volume of the Simpevarp subarea; these domains consist of mixtures of the different rock types according to Table 4-2, which is based on borehole data on the proportions of different rock types within the rock domains.

Table 4-1. Suggested transport parameters for the major rock types in the Simpevarp subarea.

Rock type	Porosity (vol %)	Formation factor (–)	K_d Sr (m^3/kg) (water type III)	K_d Cs (m^3/kg) (water type III)
Ävrö granite, Fresh (90%)	$10^{(-0.43 \pm 0.19)}$	$10^{(-3.85 \pm 0.66)}$	(4.2 ± 0.8)E–5	0.06 ± 0.03
Ävrö granite, Altered (10%)	0.33	8E–5	(1.2 ± 0.2)E–5	0.013 ± 0.006
Quartz monzodiorite, Fresh (80%)	$10^{(-0.80 \pm 0.28)}$	$10^{(-4.45 \pm 0.73)}$	(4.2 ± 0.8)E–5	0.06 ± 0.03
Quartz monzodiorite, Altered (20%)	0.33	8E–5	(1.2 ± 0.2)E–5	0.013 ± 0.006
Fine-grained dioritoid, Fresh (80%)	$10^{(-0.90 \pm 0.35)}$	$10^{(-4.69 \pm 0.89)}$	(4.2 ± 0.8)E–5	0.06 ± 0.03
Fine-grained dioritoid, Altered (20%)	0.33	8E–5	(1.2 ± 0.2)E–5	0.013 ± 0.006

Table 4-2. Estimated percentages of different rock types in the rock domains of the Simpevarp subarea.

Rock domain	Ävrö granite	Quartz monzo-diorite	Fine-grained dioritoid	Fine- to medium-grained granite	Pegmatite	Diorite and gabbro	Fine-grained mafic rock
RSMA01	76–85		9–17	1–22		0–1.7	3.0–4.9
RSMB01		0–4	91–94	1–7	0.8–1.0		0.6–0.8
RSMC01	23–34	52–74	6	2–4	0.3–1.4	0.2	1.2

4.2.2 Fractures

The following simplifications and quantitative estimates are used as a basis for the identification and parameterisation of different fracture types:

Chlorite+calcite is the overall dominating coating in the open fractures. Also hematite is present in about 20% of the open fractures in KSH01A and KSH02 and in 40% of the fractures in KSH03A. According to the core loggings, clay minerals are present in less than 5% of all open fractures, but this is probably an underestimation. Laumontites are documenteted in less than 2% of the fractures.

According to the presently available data, the presence of different fracture coatings cannot be related to specific rock types. This is important for the application of the identified fracture types in transport models; if present, such relations could provide a basis for assigning different fracture types to the different rock domains.

Concerning the host rock, it has been found that between 46 to 68% of the open fractures (according to data from KSH01–03) are situated within altered parts of the rock. If considering the nearest cm to the fracture only, this is probably an underestimation, as most of the fracture coatings documented by thin sections show hydrothermal alteration.

Based on the core mapping only, the following quantification and description of different fracture types is suggested:

A. 40% have chlorite and calcite as fracture coating (max 0.5 mm thick on each side) and fresh wall rock.

B. 20% have chlorite and calcite as fracture coating (max 0.5 mm thick on each side) and altered wall rock ≥ 5 cm (on each side of the coating).

C. 30% have chlorite+calcite+hematite as fracture coating (max 0.5 mm thick on each side); all of these fractures have altered wall rock ≥ 5 cm (on each side of the coating).

D. 10% have chlorite+calcite+clay minerals as fracture coating (max 1 mm thick on each side); all of these fractures have altered wall rock ≥ 5 cm (on each side of the coating).

The quantitative descriptions of the identified fracture types, including the available retardation parameters, are given in Tables 4-3 to 4-6. The notation “pending” frequently used in the tables indicates that this transport parameter the present geological unit is not available for this version of the site description. These gaps are intended to be filled in the later versions of the site descriptions.

Table 4-3. Retardation model for Fracture type A.

	Fracture coating	Fresh host rock
Distance	Max 0.5 mm	0.5 mm –
Porosity	Pending	According to Table 4-1
Formation factor	Pending	According to Table 4-1
Sr, K_d (m^3/kg) Groundwater type III	Pending	According to Table 4-1
Cs, K_d (m^3/kg) Groundwater type III	Pending	According to Table 4-1
Mineral content	Chlorite, calcite	See geological description
Grain size	Pending	Pending
Proportion of conducting structures	40%	
Transmissivity interval	Pending	
Direction	Pending	

Table 4-4. Retardation model for Fracture type B.

	Fracture coating	Altered wall rock	Fresh host rock
Distance	Max 0.5 mm	0.5 mm – ≥ 5 cm	≥ 5 cm –
Porosity	Pending	According to Table 4-1	According to Table 4-1
Formation factor	Pending	According to Table 4-1	According to Table 4-1
Sr, K_d (m^3/kg) Groundwater type III	Pending	According to Table 4-1	According to Table 4-1

	Fracture coating	Altered wall rock	Fresh host rock
Cs, K_d (m^3/kg) Groundwater type III	Pending	According to Table 4-1	According to Table 4-1
Mineral content	Chlorite, calcite	See geological description	See geological description
Grain size	Pending	Pending	Pending
Proportion of conducting structures	20%		
Transmissivity interval	Pending		
Direction	Pending		

Table 4-5. Retardation model for Fracture type C.

	Fracture coating	Altered wall rock	Fresh host rock
Distance	Max 0.5 mm	0.5 mm – ≥ 5 cm	≥ 5 cm –
Porosity	Pending	According to Table 4-1	According to Table 4-1
Formation factor	Pending	According to Table 4-1	According to Table 4-1
Sr, K_d (m^3/kg) Groundwater type III	Pending	According to Table 4-1	According to Table 4-1
Cs, K_d (m^3/kg) Groundwater type III	Pending	According to Table 4-1	According to Table 4-1
Mineral content	Chlorite, calcite, hematite	See geological description	See geological description
Grain size	Pending	Pending	Pending
Proportion of conducting structures	30%		
Transmissivity interval	Pending		
Direction	Pending		

Table 4-6. Retardation model for Fracture type D.

	Fracture coating	Altered wall rock	Fresh host rock
Distance	Max 1 mm	1 mm – ≥ 5 cm	≥ 5 cm –
Porosity	Pending	According to Table 4-1	According to Table 4-1
Formation factor	Pending	According to Table 4-1	According to Table 4-1
Sr, K_d (m^3/kg) Groundwater type III	Pending	According to Table 4-1	According to Table 4-1
Cs, K_d (m^3/kg) Groundwater type III	Pending	According to Table 4-1	According to Table 4-1
Mineral content	Chlorite, calcite, clay minerals	See geological description	See geological description
Grain size	Pending	Pending	Pending
Proportion of conducting structures	10%		
Transmissivity interval	Pending		
Direction	Pending		

4.2.3 Deformation zones

Local minor deformation zones

Based on the information available at this stage of the site investigation, it is not possible to provide a retardation model for the local minor deformation zones. This is due to the lack of transport data, but also to uncertainties in the evaluation of deformation zone data from the core logs. The only deterministic data available so far are for the local major deformation zones.

A few things can, however, be pointed out:

- The local minor deformation zones are hosted in altered rocks.
- Fault gouge is common, and in four zones in KSH01A and KSH02 several cm-wide gouge-filled sections hosted in metre-wide parts of cataclastic rocks are observed (e.g. at 248–250 m core length in KSH01A). Also smaller zones with only mm-thick gouge-filled fractures in altered or cataclastic rocks are observed.
- Chlorite- and clay-rich zones (on the order of < 1 cm), hosted in altered wall rock (dm-wide), are also found.
- The available data are too limited to allow conclusions on the abundances of different types of deformation zones.

Local major deformation zones

Only one local major deformation zone is penetrated by the Simpevarp boreholes, the ZSMNE0024A zone transected by borehole KSH03A at 200 m to 300 m core length. The rock is severely altered; biotite is altered to chlorite. No porosity measurements are available but a significantly higher porosity is expected in this section of the drill core. In the centre of the zone, some smaller parts are highly porous, with an episyenitic structure. Other parts are cataclastic with sections of clay-rich fault gouge (dm-wide). Hematite is a common mineral in many of the fractures in this section, together with clay minerals and chlorite.

4.3 Application of the retardation model

Tables 4-1 and 4-2 provide a basis for parameterisation of the rock domains RSMA01, RSMB01 and RSMC01. The parameterisation of each rock domain could range from a simple selection of a single parameter value for the dominant rock type in that domain to, for instance, volume averaging using data for fresh or altered rock, or both. For the diffusion parameters of the major rock types, statistical distributions are given that can be used as a basis for stochastic parameterisation of transport models.

However, no specific recommendations on the selection of data from the retardation model are given here. This implies that the present model does not provide detailed guidelines on how to “dress” the geological model with transport parameters using the parameters in the retardation model. At this stage of model development, the retardation model should be viewed as a presentation of the interpreted site-specific information on retardation parameters, intended to provide a basis for the formulation of alternative parameterisations within the Safety Assessment modelling.

The quantitative descriptions of the identified fracture types, including the available retardation parameters, are given in Tables 4-3 to 4-6. The fracture types in the present retardation model could be used as a basis for modelling radionuclide transport along flow paths in the fractured medium. However, the model could also be viewed as primarily proposing a basic structure, for discussion and further development, which from the viewpoint of numerical transport modelling will become more useful when more data are at hand.

Concerning the parameterisation of flow paths in transport models, it should also be noted that at present there are no data supporting, for instance, quantitative correlations between fracture types and hydraulic properties. Furthermore, it could be observed that the present data indicate that the presence of different fracture coatings cannot be related to specific rock types.

No identification or description of deformation zone types is given in the present model. However, the available information and indications related to the deformation zones are described in Section 4.2.3.

4.4 Evidence from process-based modelling

As discussed in Section 1.2.2, alternative retention processes and process models are considered within the site descriptive transport modelling, so far mainly in the form of process-based sorption models. It is expected that the results of this modelling will be useful for supporting, or providing alternatives to, the K_d-based sorption model regarding actual parameter values as well as for the understanding of the site-specific sorption processes in general. However, no results that can be used for these purposes are presently available.

4.5 Evaluation of uncertainties

General discussions on the uncertainties related to the site-descriptive transport model are given in the transport modelling guidelines /Berglund and Selroos, 2004/ and in the S1.1 modelling report /SKB, 2004a/. Similar to the other geoscientific disciplines, spatial variability is considered an important potential source of uncertainty in the modelling of transport properties. Quantitative results from previous studies on Äspö HRL /Byegård et al. 1998, 2001; Löfgren and Neretnieks, 2003; Xu and Wörman, 1998/, demonstrating spatial variability along flow paths and within the matrix, are briefly summarised in /SKB, 2004a/.

The main uncertainties identified in the S1.1 modelling were related to the absence of site-specific transport data. As described in the present report, this uncertainty has been partly resolved in the S1.2 model, although significant data gaps still remain. In particular, no site-specific sorption parameters were available for the S1.2 modelling. Furthermore, the available data are insufficient for establishing quantitative relations between transport parameters and other properties of fractures and deformation zones, e.g. lengths, orientations and hydraulic properties. However, it should be noted that the basis for importing transport data from Äspö HRL has been improved by the geological/mineralogical-transport evaluation undertaken as a part of the S1.2 modelling.

The uncertainties considered most relevant for the present description of transport properties can be categorised as follows:

- Uncertainties in the data and models obtained from other disciplines, primarily Geology and Hydrogeochemistry.
- Uncertainties in the interpretations and use of data and models from other disciplines, i.e. in interpretations of the relations between transport properties and various underlying properties, and the simplifications made in the identification and parameterisation of "typical" matrix materials and fractures.
- Data uncertainties related to measurements and spatial variability of transport parameters, including the "extrapolation" of small-scale measurements to relevant model scales.
- Conceptual uncertainties related to transport-specific processes and process models.

This model provides quantitative information on transport data uncertainties only. Uncertainty ranges, in most cases taken directly from the experimental data, are given in the data tables above. Essentially, these ranges incorporate both random measurement errors and the spatial variability associated with the particular dataset.

The uncertainties introduced by the inputs from other disciplines and by the "expert judgement" utilised to interpret and use these data have not been addressed in the transport description. Whereas the uncertainties in the descriptions devised by Geology and Hydrogeochemistry are discussed in the S1.2 SDM report /SKB, 2005/, Chapters 5 and 9, respectively, no attempt has been made to formulate alternative interpretations or otherwise address the "expert judgment" aspects of this work. It can be noted, however, that the differences in parameter values between, e.g. different rock types give some indications on the possible ranges of these uncertainties.

Regarding the uncertainties related to spatial variability and scale, it may be noted that all measurements providing data to the retardation model have been obtained in the laboratory, on a millimetre- to centimetre-scale. The proper means of "upscaling" these parameters is by integrating them along flow paths in groundwater flow models, implying that the scale of the flow model is the relevant model scale. The approach is here to present the data on the measurement scale, thereby providing a basis for further analysis in connection with the numerical flow and transport modelling.

5 Summary and implications for further studies

5.1 Summary of observations

Site investigation data from porosity measurements and diffusion experiments (*in situ* and in the laboratory) have been available for the S1.2 modelling. The modelling work included evaluations of data on rock mass geology, fractures and deformation zones, and hydrogeochemistry, in addition to the evaluation of transport data. The main observations from the evaluations of transport data and of data and models from other disciplines can be summarised as follows:

- Relatively large parts of the rock volumes consist of altered rock, and the proportions of altered rock show large variations among and along the boreholes. The altered rock can be assumed to have different transport properties from fresh rock.
- The open fracture frequency appears to be correlated to the altered/oxidised parts of the rock, implying that transport in the open fractures to large extent takes place in the altered parts of the rock.
- The locations of hydraulically conductive structures are mostly associated with the presence of gouge-filled faults, with outermost coatings consisting mainly of clay minerals together with calcite and pyrite grains.
- The presence of different fracture coatings is not related to the rock type in the investigated boreholes on the Simpevarp peninsula.
- Based on similarities in composition, texture and porosity, import of diffusion data from the Äspö HRL can be made by using Äspö diorite data for Ävrö granite. Diffusion data can be imported also for fine-grained granite. Due to similarities in biotite and plagioclase contents, it is proposed that Äspö diorite data are used for modelling the sorption of cation exchange sorbing nuclides on all three major rock types.

5.2 Retardation model

A retardation model was developed in accordance with the proposed modelling strategy /Widestrand et al. 2003; Berglund and Selroos, 2004/. The retardation model contains data for the fresh and altered forms of the major rock types in the Simpevarp subarea (Ävrö granite, quartz monzodiorite and fine-grained dioritoid). Specifically, the retardation model is based on porosity data from water saturation measurements on site-specific rock samples, diffusivities from formation factors measured in laboratory electrical resistivity measurements on site-specific samples, and sorption coefficients imported from Äspö HRL. The sorption dataset is limited to Cs and Sr under hydrochemical conditions corresponding to “Groundwater type III”.

Table 5-1 summarises the mean values and standard deviations (expressed as mean value ± one standard deviation) of the transport parameters of the rock mass; for further details, see Table 4-1 (in which the same porosity and formation factor data are given as log-normal distributions). It is indicated that the porosities and formation factors (normalised diffusivities) for Ävrö granite are larger than those for the other major rock types. Since the same K_d-values (obtained from experiments using Äspö diorite) are used for all three major rock types, no conclusions can be drawn on differences in sorption properties among the rock types. It can also be noted that the data uncertainty, as quantified by the standard deviations of the experimental populations, in many cases are of the same order as the mean values (or even larger).

As a basis for detailed parameterisations of the rock domains, estimated percentages of the major rock types within the rock domains RSMA01, RSMB01 and RSMC01 are presented (Table 4-2; data from Geology). Estimated proportions of fresh and altered rock for each rock type are also given. In principle, the parameterisation of each rock domain could range from a simple selection of a single parameter value representing the dominant rock type in that domain to, for instance, volume averaging using data for fresh or altered rock, or both. For the diffusion parameters of the major rock types, statistical distributions are also given.

Four different fracture types have been identified and described in the retardation model, see Tables 4-3 to 4-6. These fracture types include fractures with fracture coating on fresh rock (Fracture type A) and fractures with altered wall rock between the coating and the fresh rock (Fracture types B, C and D). The estimated percentages of the different fracture types (proportions of all open fractures) are also given. However, it should be noted that retardation parameters are not available for all materials in the model, and that quantitative relations between fracture types and other properties of the fractures (e.g. lengths, orientations and hydraulic parameters) have not been established.

Table 5-1. Summary of mean values and standard deviations of porosity, formation factor (diffusivity normalised by the free diffusivity in water) and K_d (linear equilibrium sorption coefficient) in the proposed retardation model for the fresh (non-altered) and altered forms of the major rock types.

Rock type	Porosity (vol-%)[1]	Formation factor (–)[1]	K_d Sr $(m^3/kg)^2$ (GW type III)	K_d Cs $(m^3/kg)^2$ (GW type III)	Comments
Ävrö granite (fresh)	0.40 ± 0.13	$(2.9 \pm 2.9)\times10^{-4}$	$(4.2 \pm 0.8)\times10^{-5}$	0.06 ± 0.03	Dominant rock type in RSMA01.
					One of the two dominant rock types in RSMC01.
Quartz monzo-diorite (fresh)	0.20 ± 0.13	$(1.1 \pm 1.6)\times10^{-4}$	$(4.2 \pm 0.8)\times10^{-5}$	0.06 ± 0.03	One of the two dominant rock types in RSMC01.
Fine-grained dioritoid (fresh)	0.17 ± 0.15	$(1.0 \pm 1.7)\times10^{-4}$	$(4.2 \pm 0.8)\times10^{-5}$	0.06 ± 0.03	Dominant rock type in RSMB01.
Altered rock	0.33[3]	$(0.8 \pm 0.4)\times10^{-4}$	$(1.2 \pm 0.2)\times10^{-5}$	0.013 ± 0.006	The same parameter values are assumed for the altered forms of all major rock types.

[1] Site investigation data (except for the altered rock data).
[2] Based on data from Äspö HRL (further evaluated in the site descriptive modelling).
[3] Only one value available.

Although somewhat limited in terms of data and correlations to other parameters and properties of the system, the presented model can be used as a basis for parameterisation of numerical transport models and, perhaps more important, as a basic structure that can be subject to further discussions and development. Concerning the parameterisation of transport models, it could be observed that the present data show that the presence of different fracture coatings cannot be related to specific rock types. No identification or description of fracture zone types is given in the present model. However, the available information and indications related to fracture zones are described in Section 4.2.3.

5.3 Implications for further studies

The present summary and evaluation of site-specific retardation data from Simpevarp shows that some types of site data still are missing in the site database. In particular, no site investigation data on sorption parameters are available. However, a large number of samples have been taken from the Simpevarp and Laxemar rock cores. Laboratory experiments for determining sorption parameters, and additional porosities and diffusion data, are under way, and additional *in situ* measurements have been performed.

This means that the site-specific database will be considerably improved during 2005–2006, filling many of the data gaps identified in the S1.2 model. However, the additional amount of data contained in the Laxemar 1.2 data freeze is expected to be relatively small. For the Laxemar 1.2 modelling, it is therefore proposed that an extraction of data from on-going experiments is made, similar to the one in Simpevarp 1.2, in order to improve the database and the resulting model.

Altered and intact varieties of the same rock type may have significantly different transport properties. More data and modelling are needed in order to verify or exclude such differences. The on-going site investigation programme will provide more data on altered and fracture-filling materials, which improves the basis for parameterisation of fractures and deformation zones. It should be noted, however, that the present Safety Assessment transport modelling uses retardation parameters for intact (non-altered) rock. Therefore, this modelling is not directly dependent on the availability of parameters for fracture coatings and altered rock.

An important consideration is the potential role of the fine- to medium-grained granite. This is a minor rock type within the Simpevarp subarea. Based on experiences from Äspö HRL, however, the fine-grained granite may host a relatively larger percentage of conductive fractures, which implies that its importance is larger than indicated by its volumetric proportion of the host rock. Whether this observation is applicable also to the Laxemar and Simpevarp subareas is not evaluated in the present modelling, but this issue should be addressed in Laxemar 1.2.

The nomenclature concerning fractures and deformation zones needs to be discussed in connection with forthcoming modelling activities, especially for the identification and parameterisation of fracture and zone types. The single fractures can be described in a relatively simple manner, whereas the local minor zones may need a subdivision as they are defined as zones with lengths of 10 m to 1,000 m. The separation of fractures and smaller deformation zones is also difficult, and the criteria guiding this separation need to be discussed.

6 References

Berglund S, Selroos J-O, 2004. Transport properties site descriptive model – Guidelines for evaluation and modelling. SKB R-03-09. Svensk Kärnbränslehantering AB.

Brunauer S, Emmet P H, Teller E, 1938. Adsorption of gases in multimolecular layers. J. Am Chem Soc, 60: 309–319.

Byegård J, Johansson H, Skålberg M, Tullborg E-L, 1998. The interaction of sorbing and non-sorbing tracers with different Äspö rock types – Sorption and diffusion experiments in the laboratory scale. SKB TR 98-18. Svensk Kärnbränslehantering AB.

Byegård J, Widestrand H, Skålberg M, Tullborg E-L, Siitari-Kauppi M, 2001. Complementary investigation of diffusivity, porosity and sorptivity of Feature A-site specific geological material. SKB ICR-01-04. Svensk Kärnbränslehantering AB.

Carbol P, Engkvist I, 1997. Compilation of radionuclide sorption coefficients for performance assessment. SKB R-97-13. Svensk Kärnbränslehantering AB.

Dershowitz W, Winberg A, Hermanson J, Byegård J, Tullborg E-L, Andersson P, Mazurek M, 2003. Äspö Hard Rock Laboratory. Äspö Task Force on modelling of groundwater flow and transport of solutes – Task 6C – A semi-synthetic model of block scale conductive structures at the Äspö HRL. SKB IPR-03-13. Svensk Kärnbränslehantering AB.

Drake H, Tullborg E-L, 2004. Oskarshamn site investigation. Fracture mineralogy and wall rock alteration. Results from drill core KSH01A+B. SKB P-04-250. Svensk Kärnbränslehantering AB.

Eliasson T, 1993. Mineralogy, geochemistry and petrophysics of red coloured granite adjacent to fractures. SKB TR-93-06. Svensk Kärnbränslehantering AB.

Gustavsson E, Gunnarsson M, 2005. Oskarshamn site investigation. Laboratory data from the site investigation programme for the transport properties of the rock. Boreholes KSH01A, KSH02A and KLX02A. SKB P-05-18. Svensk Kärnbränslehantering AB.

Hellmuth K H, Lukkarinen S, Siitari-Kauppi M, 1994. Rock matrix studies with carbon-14-polymethylmethacrylate (PMMA). Method, development and applications. Isotopenpraxis Environ. Health Stud., 30: 47–60.

Hellmuth K H, Siitari-Kauppi M, Lindberg A, 1993. Study of porosity and migration pathways in crystalline rock by impregnation with ^{14}C-polymethylmethacrylate. J. Cont. Hydrol., 13: 403–418.

Jakobsson A-M, 1999. Measurement and modelling using surface complexation of cation (II to IV) sorption onto mineral oxides. Ph.D. Thesis. Chalmers University of Technology, Department of Nuclear Chemistry, Göteborg, Sweden.

Johansson H, Byegård J, Skarnemark G, Skålberg M, 1997. Matrix diffusion of some alkali and alkaline earth metals in granitic rock. Mat. Res. Soc. Symp. Proc. 465: 871–878.

Landström O, Tullborg E-L, 1993. Results from a geochemical study of zone NE-1, based on samples from the Äspö tunnel and drillcore KAS 16 (395 to 451 m). SKB Progress Report 25-93-01. Svensk Kärnbränslehantering AB.

Li Y-H, Gregory S, 1974. Diffusion of ions in sea water and in deep sea sediments, Geochim. et Cosmochim. Acta 47: 703–714.

Löfgren M, Neretnieks I, 2003. Formation factor logging by electrical methods. Comparison of formation factor logs obtained *in situ* and in the laboratory. J. Contam. Hydrol. 61: 107–115.

Löfgren M, Neretnieks I, 2005. Oskarshamn site investigation. Formation factor logging in-situ and in the laboratory by electrical methods in KSH01A and KSH02. Measurements and evaluation of methodology. SKB P-05-27. Svensk Kärnbränslehantering AB.

Mazurek M, Bossart P, Eliasson T, 1997. Classification and characterisation of water conduction features at Äspö: Results of investigations on the outcrop scale. SKB ICR-97-01. Svensk Kärnbränslehantering AB.

Munier R, 1993. Segmentation, fragmentation and jostling of the Baltic shield with time. Ph.D. Thesis, Acta Universitatus Upsaliensis 37. University of Uppsala, Uppsala, Sweden.

Ohlsson Y, Neretnieks I, 1997. Diffusion data in granite – Recommended values. SKB TR-97-20. Svensk Kärnbränslehantering AB.

Poteri A, Billaux D, Dershowitz W, Gomez-Hernandez JJ, Cvetkovic V, Hautojärvi A, Holton D, Medina A, Winberg A (ed.), 2002. Final report of the TRUE Block Scale project. 3. Modelling of flow and transport. SKB TR-02-15. Svensk Kärnbränslehantering AB.

SKB, 2004a. Preliminary site description. Simpevarp area – version 1.1. SKB R-04-25. Svensk Kärnbränslehantering AB.

SKB 2004b. Hydrogeochemical evaluation for Simpevarp model version 1.2. Preliminary site description of the Simpevarp area. SKB R-04-74. Svensk Kärnbränslehantering AB.

SKB, 2005. Preliminary site description. Simpevarp subarea – version 1.2. SKB R-05-08. Svensk Kärnbränslehantering AB.

Stråhle A, 2001. Definition och beskrivning av parametrar för geologisk, geofysisk och bergmekanisk kartering av berget. SKB R-01-19. Svensk Kärnbränslehantering AB.

Tullborg E-L, 1995. Mineralogical and chemical data on rocks and fracture minerals from Äspö. SKB Äspö Hard Rock Laboratory Technical note 25-95-07g. Svensk Kärnbränslehantering AB.

Widestrand H, Byegård J, Ohlsson Y, Tullborg E-L, 2003. Strategy for the use of laboratory methods in the site investigations programme for the transport properties of the rock. SKB R-03-20. Svensk Kärnbränslehantering AB.

Winberg A, Hermansson J, Tullborg, E-L, Staub, I, 2003. Äspö Hard Rock Laboratory. Long term diffusion experiment, Structural model of the LTDE site and detailed description of the characteristics of the experimental volume including target structure and intact rock section. SKB IPR-03-51. Svensk Kärnbränslehantering AB.

Winberg A, Andersson P, Hermansson J, Byegård J, Cvetkovic V, Birgersson L, 2000. Äspö Hard Rock Laboratory. Final report on the first stage of the tracer retention understanding experiments. SKB TR-00-07. Svensk Kärnbränslehantering AB.

Xu S, Wörman A, 1998. Statistical Patterns of Geochemistry in Crystalline Rock and Effect of Sorption Kinetics on Radionuclide Migration. SKI Technical Report 98:41. Statens kärnkraftinspektion.

Appendix 1

Porosity data

The results of porosity measurements on samples taken for laboratory through-diffusion and batch sorption experiments are presented in Table A1-1 (KSH01A) and Table A1-2 (KSH02).

Table A1-1. Porosity data from KSH01A.

ID code	Secup	Seclow	Rock_type	Porosity (%)
KSH01A	19.96	19.99	Quartz monzodiorite	0.47
KSH01A	39.59	39.62	Quartz monzodiorite	0.10
KSH01A	59.12	59.15	Quartz monzodiorite	0.08
KSH01A	76.65	76.68	Quartz monzodiorite	0.12
KSH01A	99.71	99.74	Quartz monzodiorite	0.08
KSH01A	121.41	121.44	Quartz monzodiorite	0.08
KSH01A	140.68	140.71	Quartz monzodiorite	0.34
KSH01A	160.72	160.75	Quartz monzodiorite	0.10
KSH01A	181.47	181.50	Quartz monzodiorite	0.13
KSH01A	200.11	200.14	Quartz monzodiorite	0.08
KSH01A	219.36	219.39	Fine-grained dioritoid	0.08
KSH01A	222.72	222.73	Fine-grained dioritoid	0.15
KSH01A	222.73	222.76	Fine-grained dioritoid	0.08
KSH01A	239.96	239.99	Fine-grained dioritoid	0.19
KSH01A	261.08	261.11	Quartz monzodiorite	1.59
KSH01A	280.23	280.26	Quartz monzodiorite	0.45
KSH01A	295.41	295.44	Quartz monzodiorite	0.13
KSH01A	317.78	317.81	Quartz monzodiorite	0.08
KSH01A	340.88	340.91	Quartz monzodiorite	0.08
KSH01A	362.55	362.58	Fine-grained granite	0.12
KSH01A	378.98	379.01	Fine-grained dioritoid	0.08
KSH01A	398.75	398.78	Fine-grained dioritoid	0.13
KSH01A	420.78	420.81	Fine-grained dioritoid	0.41
KSH01A	440.23	440.26	Fine-grained dioritoid	0.75
KSH01A	460.00	460.05	Fine-grained dioritoid	0.20
KSH01A	478.20	478.25	Fine-grained dioritoid	0.07
KSH01A	500.30	500.35	Fine-grained dioritoid	0.24
KSH01A	520.75	520.80	Fine-grained dioritoid	0.15
KSH01A	539.00	539.05	Fine-grained dioritoid	0.10
KSH01A	559.90	559.95	Fine-grained dioritoid	0.07
KSH01A	580.87	580.92	Fine-grained dioritoid	0.13
KSH01A	598.65	598.70	Fine-grained dioritoid	0.13
KSH01A	620.22	620.27	Fine-grained dioritoid	0.41
KSH01A	640.55	640.60	Ävrö granite	0.17
KSH01A	661.06	661.11	Ävrö granite	0.12

ID code	Secup	Seclow	Rock_type	Porosity (%)
KSH01A	680.20	680.25	Fine-grained granite	0.05
KSH01A	699.00	699.05	Fine-grained granite	0.02
KSH01A	720.24	720.29	Fine-grained granite	0.20
KSH01A	760.75	760.80	Quartz monzodiorite	0.12
KSH01A	779.19	779.24	Ävrö granite	0.19
KSH01A	800.40	800.45	Fine-grained dioritoid	0.58
KSH01A	820.08	820.13	Ävrö granite	0.47
KSH01A	840.70	840.75	Ävrö granite	0.35
KSH01A	859.15	859.20	Fine-grained granite	0.30
KSH01A	880.50	880.55	Ävrö granite	0.39
KSH01A	891.66	891.67	Ävrö granite	0.58
KSH01A	891.67	891.68	Ävrö granite	0.54
KSH01A	891.69	891.72	Ävrö granite	0.45
KSH01A	891.72	891.77	Ävrö granite	0.43
KSH01A	891.77	891.78	Ävrö granite	0.48
KSH01A	891.78	891.79	Ävrö granite	0.60
KSH01A	891.80	891.83	Ävrö granite	0.44
KSH01A	891.83	891.88	Ävrö granite	0.42
KSH01A	891.88	891.89	Ävrö granite	0.48
KSH01A	891.89	891.90	Ävrö granite	0.44
KSH01A	891.91	891.94	Ävrö granite	0.46
KSH01A	898.60	898.65	Ävrö granite	0.35
KSH01A	919.65	919.70	Ävrö granite	0.24
KSH01A	940.80	940.85	Ävrö granite	0.32
KSH01A	960.77	960.82	Quartz monzodiorite	0.35
KSH01A	980.40	980.45	Quartz monzodiorite	0.25
KSH01A	981.43	981.46	Quartz monzodiorite	0.29
KSH01A	981.46	981.49	Quartz monzodiorite	0.29
KSH01A	981.50	981.53	Quartz monzodiorite	0.27
KSH01A	999.45	999.50	Quartz monzodiorite	0.22

Table A1-2. Porosity data from KSH02.

ID code	Secup	Seclow	Rock_type	Porosity (%)
KSH02	19.96	19.99	Fine-grained dioritoid	0.05
KSH02	39.96	39.99	Fine-grained dioritoid	0.07
KSH02	60.18	60.21	Fine-grained dioritoid	0.20
KSH02	80.01	80.04	Fine-grained dioritoid	0.12
KSH02	99.91	99.94	Fine-grained dioritoid	0.53
KSH02	119.96	119.99	Fine-grained dioritoid	0.10
KSH02	140.16	140.19	Fine-grained dioritoid	0.08
KSH02	148.09	148.10	Fine-grained dioritoid	0.38
KSH02	148.11	148.12	Fine-grained dioritoid	0.15

ID code	Secup	Seclow	Rock_type	Porosity (%)
KSH02	148.12	148.15	Fine-grained dioritoid	0.07
KSH02	148.16	148.21	Fine-grained dioritoid	0.06
KSH02	148.21	148.22	Fine-grained dioritoid	0.00
KSH02	148.23	148.24	Fine-grained dioritoid	0.05
KSH02	148.24	148.27	Fine-grained dioritoid	0.08
KSH02	148.28	148.33	Fine-grained dioritoid	0.02
KSH02	148.34	148.35	Fine-grained dioritoid	0.05
KSH02	148.36	148.39	Fine-grained dioritoid	0.05
KSH02	148.39	148.44	Fine-grained dioritoid	0.03
KSH02	159.96	159.99	Fine-grained dioritoid	0.20
KSH02	179.96	179.99	Fine-grained dioritoid	0.10
KSH02	219.66	219.69	Fine-grained dioritoid	0.12
KSH02	239.96	239.99	Fine-grained dioritoid	0.07
KSH02	259.83	259.86	Fine-grained dioritoid	0.05
KSH02	280.01	280.04	Fine-grained dioritoid	0.07
KSH02	299.95	299.98	Fine-grained dioritoid	0.34
KSH02	339.94	339.97	Fine-grained dioritoid	0.10
KSH02	360.06	360.09	Fine-grained dioritoid	0.68
KSH02	419.96	419.99	Fine-grained dioritoid	0.84
KSH02	459.69	459.72	Fine-grained dioritoid	0.27
KSH02	474.46	474.47	Fine-grained dioritoid	0.61
KSH02	474.47	474.48	Fine-grained dioritoid	0.40
KSH02	474.56	474.59	Fine-grained dioritoid	0.42
KSH02	474.60	474.65	Fine-grained dioritoid	0.10
KSH02	474.65	474.66	Fine-grained dioritoid	0.30
KSH02	474.66	474.67	Fine-grained dioritoid	0.20
KSH02	474.68	474.71	Fine-grained dioritoid	0.20
KSH02	474.71	474.76	Fine-grained dioritoid	0.31
KSH02	474.77	474.78	Fine-grained dioritoid	0.59
KSH02	474.78	474.79	Fine-grained dioritoid	0.47
KSH02	474.80	474.83	Fine-grained dioritoid	0.18
KSH02	474.86	474.91	Fine-grained dioritoid	0.42
KSH02	480.01	480.04	Fine-grained dioritoid	0.19
KSH02	500.01	500.04	Fine-grained dioritoid	1.33
KSH02	539.86	539.89	Fine-grained dioritoid	0.20
KSH02	560.06	560.09	Fine-grained dioritoid	0.21
KSH02	580.11	580.14	Fine-grained granite	0.07
KSH02	599.35	599.36	Fine-grained granite	0.32
KSH02	599.36	599.37	Fine-grained granite	0.28
KSH02	599.37	599.40	Fine-grained granite	0.19
KSH02	599.41	599.46	Fine-grained granite	0.20
KSH02	599.46	599.47	Fine-grained granite	0.23
KSH02	599.47	599.48	Fine-grained granite	0.26
KSH02	599.48	599.51	Fine-grained granite	0.19
KSH02	599.52	599.57	Fine-grained granite	0.24

ID code	Secup	Seclow	Rock_type	Porosity (%)
KSH02	599.57	599.58	Fine-grained granite	0.40
KSH02	599.58	599.59	Fine-grained granite	0.25
KSH02	599.59	599.62	Fine-grained granite	0.29
KSH02	599.62	599.67	Fine-grained granite	0.24
KSH02	600.01	600.04	Fine-grained granite	0.17
KSH02	639.89	639.92	Fine-grained granite	0.30
KSH02	660.09	660.12	Fine-grained dioritoid	0.09
KSH02	680.16	680.19	Fine-grained dioritoid	0.31
KSH02	685.98	685.99	Fine-grained dioritoid	0.38
KSH02	685.99	686.00	Fine-grained dioritoid	0.25
KSH02	686.00	686.03	Fine-grained dioritoid	0.10
KSH02	686.04	686.09	Fine-grained dioritoid	0.08
KSH02	686.09	686.10	Fine-grained dioritoid	0.19
KSH02	686.10	686.11	Fine-grained dioritoid	0.25
KSH02	686.11	686.14	Fine-grained dioritoid	0.12
KSH02	686.15	686.20	Fine-grained dioritoid	0.04
KSH02	686.20	686.21	Fine-grained dioritoid	0.10
KSH02	686.21	686.22	Fine-grained dioritoid	0.05
KSH02	686.22	686.25	Fine-grained dioritoid	0.05
KSH02	686.26	686.31	Fine-grained dioritoid	0.05
KSH02	700.01	700.04	Fine-grained granite	0.20
KSH02	720.01	720.04	Fine-grained dioritoid	0.10
KSH02	740.01	740.04	Fine-grained granite	1.15
KSH02	760.17	760.20	Fine-grained dioritoid	0.14
KSH02	779.82	779.85	Fine-grained dioritoid	0.25
KSH02	819.91	819.94	Fine-grained dioritoid	0.42
KSH02	840.01	840.04	Fine-grained dioritoid	0.02
KSH02	859.96	859.99	Fine-grained dioritoid	0.21
KSH02	880.01	880.04	Fine-grained dioritoid	0.15
KSH02	900.01	900.04	Fine-grained dioritoid	0.17
KSH02	920.01	920.04	Fine-grained dioritoid	0.13
KSH02	940.01	940.04	Fine-grained dioritoid	0.13
KSH02	959.96	959.99	Fine-grained dioritoid	0.12
KSH02	979.96	979.99	Mafic rock, fine-grained	0.20

Appendix 2

Formation factors and associated porosities

Laboratory and *in situ* formation factors (Fm) and porosities measured on samples used in laboratory formation factor measurements are presented in Table A2-1 (KSH01A) and Table A2-2 (KSH02).

Table A2-1. Formation factor and porosity data from KSH01A. The yellow fields indicate measurement levels where both laboratory and *in situ* data are available.

Borehole length (m)	Fm laboratory	Fm in-situ	Rock type	Porosity (%)
19.95	1.56×10^{-4}		Quartz monzodiorite	0.47
59.11	2.06×10^{-5}		Quartz monzodiorite	0.08
79.64	2.31×10^{-5}		Quartz monzodiorite	0.12
99.70	2.40×10^{-5}		Quartz monzodiorite	0.08
121.40	7.28×10^{-6}		Quartz monzodiorite	0.08
160.71	8.49×10^{-6}	1.46×10^{-5}	Quartz monzodiorite	0.1
181.46	5.28×10^{-5}	1.46×10^{-5}	Quartz monzodiorite	0.13
200.10	2.08×10^{-6}	4.43×10^{-5}	Quartz monzodiorite	0.08
239.95	6.15×10^{-6}		Fine-grained dioritoid	0.19
261.07	4.12×10^{-4}		Quartz monzodiorite	1.59
295.40	3.47×10^{-5}		Quartz monzodiorite	0.13
317.77	6.92×10^{-5}	1.40×10^{-5}	Quartz monzodiorite	0.08
340.87	1.61×10^{-6}	1.14×10^{-5}	Quartz monzodiorite	0.08
362.54	1.14×10^{-5}		Ävrö granite	0.12
378.97	1.40×10^{-5}		Fine-grained dioritoid	0.08
398.74	1.17×10^{-5}		Fine-grained dioritoid	0.13
420.77	2.47×10^{-5}		Fine-grained dioritoid	0.41
440.22	3.46×10^{-4}		Fine-grained dioritoid	0.75
460.00	4.48×10^{-4}	1.84×10^{-5}	Fine-grained dioritoid	0.2
478.20	1.63×10^{-6}		Fine-grained dioritoid	0.07
500.30	2.53×10^{-5}	1.49×10^{-5}	Fine-grained dioritoid	0.24
520.75	4.29×10^{-6}		Fine-grained dioritoid	0.15
539.00	1.95×10^{-6}		Fine-grained dioritoid	0.1
559.90	1.34×10^{-6}		Fine-grained dioritoid	0.07
580.87	4.66×10^{-6}		Fine-grained dioritoid	0.13
598.65	2.48×10^{-5}		Fine-grained dioritoid	0.13
620.22	1.95×10^{-4}		Fine-grained dioritoid	0.41
640.55	4.64×10^{-5}	2.43×10^{-5}	Ävrö granite	0.17
661.06	1.87×10^{-5}		Ävrö granite	0.12
680.20	5.87×10^{-6}		Fine-grained granite	0.05
699.00	9.06×10^{-6}		Pegmatite	0.02
720.24	8.82×10^{-5}		Fine-grained granite	0.2
740.53	1.56×10^{-5}	2.38×10^{-5}	Quartz monzodiorite	0.12
760.75	1.46×10^{-5}		Quartz monzodiorite	0.12
779.19	6.03×10^{-5}	3.91×10^{-5}	Quartz monzodiorite	0.19

Borehole length (m)	Fm laboratory	Fm in-situ	Rock type	Porosity (%)
800.40	1.49×10^{-4}	1.18×10^{-4}	Ävrö granite	0.58
820.08	9.04×10^{-4}	1.27×10^{-4}	Ävrö granite	0.47
840.70	4.70×10^{-4}	5.50×10^{-5}	Ävrö granite	0.35
859.15	4.88×10^{-4}		Fine-grained granite	0.3
880.50	3.84×10^{-4}		Ävrö granite	0.39
898.60	3.29×10^{-4}	4.77×10^{-5}	Ävrö granite	0.35
919.65	2.91×10^{-4}		Ävrö granite	0.24
960.77	5.72×10^{-4}	1.84×10^{-5}	Quartz monzodiorite	0.35
980.40	2.73×10^{-4}	1.62×10^{-5}	Quartz monzodiorite	0.25
999.45	2.19×10^{-4}	1.53×10^{-5}	Quartz monzodiorite	0.22

Table A2-2. Formation factor and porosity data from KSH02. The yellow fields indicate measurement levels where both laboratory and *in situ* data are available.

Borehole length (m)	Fm laboratory	Fm in-situ	Rock type	Porosity (%)
19.95	2.88×10^{-7}		Fine-grained dioritoid	0.05
39.95	2.20×10^{-6}		Fine-grained dioritoid	0.07
60.17	2.36×10^{-5}		Fine-grained dioritoid	0.20
80.00	8.22×10^{-5}		Fine-grained dioritoid	0.12
99.90	1.76×10^{-4}		Fine-grained dioritoid	0.53
119.95	3.76×10^{-6}		Fine-grained dioritoid	0.10
140.15	1.63×10^{-6}		Fine-grained dioritoid	0.08
159.95	2.31×10^{-5}		Fine-grained dioritoid	0.20
179.95	7.85×10^{-6}		Fine-grained dioritoid	0.10
219.65	1.12×10^{-6}		Fine-grained dioritoid	0.12
239.15	2.89×10^{-6}		Fine-grained dioritoid	0.07
259.82	6.93×10^{-6}		Fine-grained dioritoid	0.05
280.00	2.31×10^{-6}		Fine-grained dioritoid	0.07
360.05	5.26×10^{-4}		Fine-grained dioritoid	0.68
399.95	1.06×10^{-5}		Fine-grained dioritoid	
419.95	2.26×10^{-4}		Fine-grained dioritoid	0.84
439.95	3.06×10^{-6}	2.96×10^{-5}	Fine-grained dioritoid	
459.68	1.72×10^{-4}		Fine-grained dioritoid	0.27
500.37	8.40×10^{-4}		Fine-grained dioritoid	1.33
539.85	2.33×10^{-5}		Fine-grained dioritoid	0.20
560.05	1.64×10^{-5}		Fine-grained dioritoid	0.21
580.10	2.17×10^{-7}		Fine-grained granite	0.07
639.88	1.93×10^{-4}		Fine-grained granite	0.30
680.15	3.16×10^{-5}		Fine-grained dioritoid	0.31
700.00	1.75×10^{-4}		Fine-grained granite	0.20
720.00	1.56×10^{-6}		Fine-grained dioritoid	0.10
740.00	3.66×10^{-4}		Fine-grained granite	1.15
760.16	9.39×10^{-6}		Fine-grained dioritoid	0.14

Borehole length (m)	Fm laboratory	Fm in-situ	Rock type	Porosity (%)
779.81	3.46×10^{-4}		Fine-grained dioritoid	0.25
819.90	4.06×10^{-4}		Fine-grained dioritoid	0.42
840.00	1.87×10^{-6}	4.81×10^{-6}	Fine-grained dioritoid	0.02
859.95	5.09×10^{-5}		Fine-grained dioritoid	0.21
880.00	1.27×10^{-4}	4.82×10^{-6}	Fine-grained dioritoid	0.15
900.00	9.17×10^{-5}	7.47×10^{-6}	Fine-grained dioritoid	0.17
920.00	7.40×10^{-5}	5.31×10^{-6}	Fine-grained dioritoid	0.13
940.00	1.48×10^{-4}	5.29×10^{-6}	Fine-grained dioritoid	0.13
959.95	9.35×10^{-5}		Fine-grained dioritoid	0.12
979.95	7.41×10^{-5}	2.00×10^{-5}	Mafic rock, fine-grained	0.20